6th Dynamics Days Central Asia

On a nonholonomic system similar to the Chaplygin sphere

A.V. Borisov

2020

1. Let us consider in more detail the Chaplygin ball problem. We recall that the Chaplygin ball is a spherical rigid body in which the principal moments of inertia are different and the center of mass is at the geometric center. For the first time this problem was explicitly integrated by S. A. Chaplygin [29] in 1903. In this case, the equations of motion have an invariant measure, preserve energy and the angular momentum vector referred to the axes of a fixed coordinate system. This case is similar to the Euler case in rigid body dynamics and can be exactly reduced to it if the angular momentum lies in the direction perpendicular to the horizontal plane [29, 14].

However, in contrast to the Euler case, (reduced) equations of motion are represented in Hamiltonian form only after rescaling time [22]. An explicit representation in conformally Hamiltonian form is presented in [23], and some justification of the found representation is discussed in [2]. An analysis of trajectories of the point of contact of the Chaplygin ball on a plane is presented in [13].

2. In connection with the development of the methods of nonholonomic mechanics and possible applications of rolling balls to robotics, various versions of the Chaplygin ball rolling problem are considered:

- addition of *gyrostatic momentum* [48] and *the Brun field* [44];
- rolling in a *spherical suspension* (BMF system) [10, 9], a *ball suspension* [37, 14] and *on a uniformly rotating plane* [51, 35, 3, 11];
- addition of *a fluid-filled cavity* to the ball [21].

We also highlight a new spectrum of problems which involve considering another nonholonomic model. In addition to assuming that the velocity of the point of contact is zero, this model assumes that the projection of the angular velocity onto the normal to the plane is also zero (i.e., there is no spinning). In [34] it is proposed to implement this model by coating the rolling body with sufficiently soft rubber (see also [42]). This is why it is also called the *rubber rolling model*.

Within the rubber model the Chaplygin ball rolling problem is integrable and is addressed in [27, 19]. It has turned out that in the case of the Chaplygin ball there exists an interrelation between the rubber rolling model and the standard (classical) model of rolling without slipping with the possibility of spinning: the trajectories of the reduced system for the Chaplygin ball turn out to be transversal (to each other) windings of the same tori [8, 52].

3. Of particularly great interest from the viewpoint of control theory and various applications [12] are problems of the rolling of a ball with periodically varying mass distribution, which is caused by the control mechanism placed inside the ball [49, 41, 43]. The qualitative analysis of such systems is complicated by the fact that they reduce to investigating a Poincaré map, which defies visualization (since its dimension is greater than three). Moreover, the reduced equations of motion explicitly depend on time, which makes the stability analysis of particular motions difficult.

One of the simplest examples of such systems is the (toy) beaver ball[1] (see Fig. 1). It is a spherical shell inside which a rigid body (rotor, frame) rotates with constant angular velocity about the axis passing through the geometric center of the sphere. The body is fastened in such a way that its center of mass does not lie on the axis of rotation. As a result, the center of mass of the entire system is displaced relative to the geometric center of the shell and executes periodic motion. In [41] this influence of the rigid body is modeled using a material point which moves in a circle, and the analysis of the equations of motion thus obtained is confined to numerically constructing the trajectory of the point of contact and the time dependence of the angular velocity of the ball for fixed initial conditions and parameters.

---

[1] The use of the word *beaver* is due to the fact that commercial variants have a furry toy fastened on the outer side of the sphere.

Fig. 1 : Beaver ball in dismantled form.

It has recently been shown [4, 43, 5, 6] that nonholonomic systems with periodically varying mass distribution may exhibit motions where the velocity of the carrying body increases indefinitely. In contrast to Hamiltonian systems (see, e. g., [47]), the indefinite increase in the velocity is characteristic of systems that reduce to a two-dimensional map which is no longer area-preserving.

4. We consider the problem of the rolling of a dynamically symmetric spherical shell with a frame (rigid body) which rotates along its symmetry axis and on which rotors (gyrostats) are fastened. It is assumed that the center of mass of the entire system is at the geometric center of the ball. This case arises, for example, if one places the rigid body inside the shell of the beaver ball in such a way that its center of mass is at the geometric center of the shell (balanced beaver ball).

Generally speaking, the analysis of dynamical equations of an (unbalanced) beaver ball is complicated by the large dimension of the Poincaré map. For the system under consideration, the problem is reduced, by using additional integrals, to investigating of a two-dimensional Poincaré map. We present the main results obtained in this study:

— Equations of motion are obtained which describe the rolling without slipping (for the classical rolling model and the rubber rolling model) of a robot with a spherical shell. In the case of constant velocity of rotation of the shell relative to the frame (capsule), a representation of the equations of motion in the form of an autonomous system is found which is a generalization of the nonholonomic system in the Chaplygin ball problem (see Section 2). In this case, however, these equations have no continuous invariant measure and no energy integral.

- Conservation laws (first integrals) are found and it is shown that on the corresponding integral surface (which turns out to be three-dimensional) the analysis of the reduced system can be carried out using a two-dimensional Poincaré map (see Section 3).
- A qualitative analysis for the rubber rolling model is carried out in the case of motion of the system from rest. In particular, a stability analysis is made of partial solutions that correspond to the fixed points of the reduced system. The asymptotic nature of the behavior of the system in a neighborhood of these solutions suggests that that there is no continuous invariant measure. This is indicative of a considerable difference of this system from the Chaplygin ball problem and its various generalizations (see Section 4).
- Partial solutions are found for which the internal frame (capsule) remains fixed relative to the supporting surface, and conditions for their stability (gyroscopic stabilization) are analyzed (see Section 5.1).
- It is shown that at certain parameter values the system may exhibit irregular (chaotic) behavior.
  In this case, a strange attractor arises in the phase space of the reduced system (see Section 5.2).

The beaver ball is of interest to children, since it exhibits interesting dynamical behavior — it moves chaotically on the plane and behaves particularly strangely when colliding with obstacles. For the system considered in this paper, problems of chaotic behavior in the reduced phase space and of the behavior of the point of contact are only touched upon. Yet these problems, which are undoubtedly of interest, require a more detailed investigation of the resulting system.

2. EQUATIONS OF MOTION

Consider a system moving on a horizontal plane and consisting of several bodies (see Fig. 3):

1) a dynamically symmetric *spherical shell* in which the center of mass is at the geometric center;
2) a *frame,*[2] a rigid body with an arbitrary mass distribution, which is fastened inside the shell by means of cylindrical hinges. The frame is able to rotate relative to the shell with a given angular velocity $\boldsymbol{\Omega}(t)$;
3) n dynamically symmetric rigid bodies (*rotors*) which are fastened on the frame.

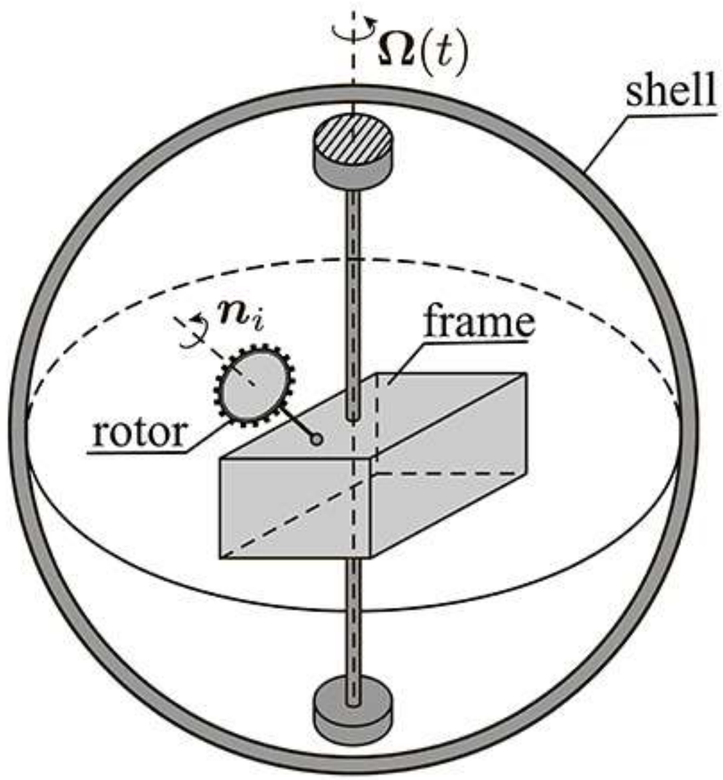

Fig. 3: Structure of the system for one rotor ($n = 1$).

[2] As a rule, it is the frame that is of the greatest technical importance in mobile devices, since devices for observations, life-support capsules etc. can be connected with it. Therefore, its stabilization relative to the fixed coordinate system is a high-priority problem.

We assume that the frame and the rotors are located inside the spherical shell in such a way that *the center of mass of the entire system is at the geometric center of the shell*, that is, we consider a balanced case.

Suppose that the frame and the rotors execute the following motion relative to the shell:

- the frame rotates with angular velocity $\boldsymbol{\Omega}(t)$, given as a function of time, about the axis of dynamical symmetry of the shell. If the shell is homogeneous, then any straight line passing through the geometric center of the shell can be chosen as the axis of rotation of the frame;
- the rotors rotate (relative to the frame) with angular velocity $\dot{\phi}_i(t)$, given as a function of time, about its axis of dynamical symmetry $\boldsymbol{n}_i$.

We define two coordinate systems (see Fig. 4):

- an *inertial* coordinate system $OXYZ$ with origin at some point of the plane and with the axis OZ perpendicular to it.
- a *noninertial* coordinate system $Cx_1x_2x_3$, which is attached to the frame, so that the origin C coincides with the center of mass of the system.

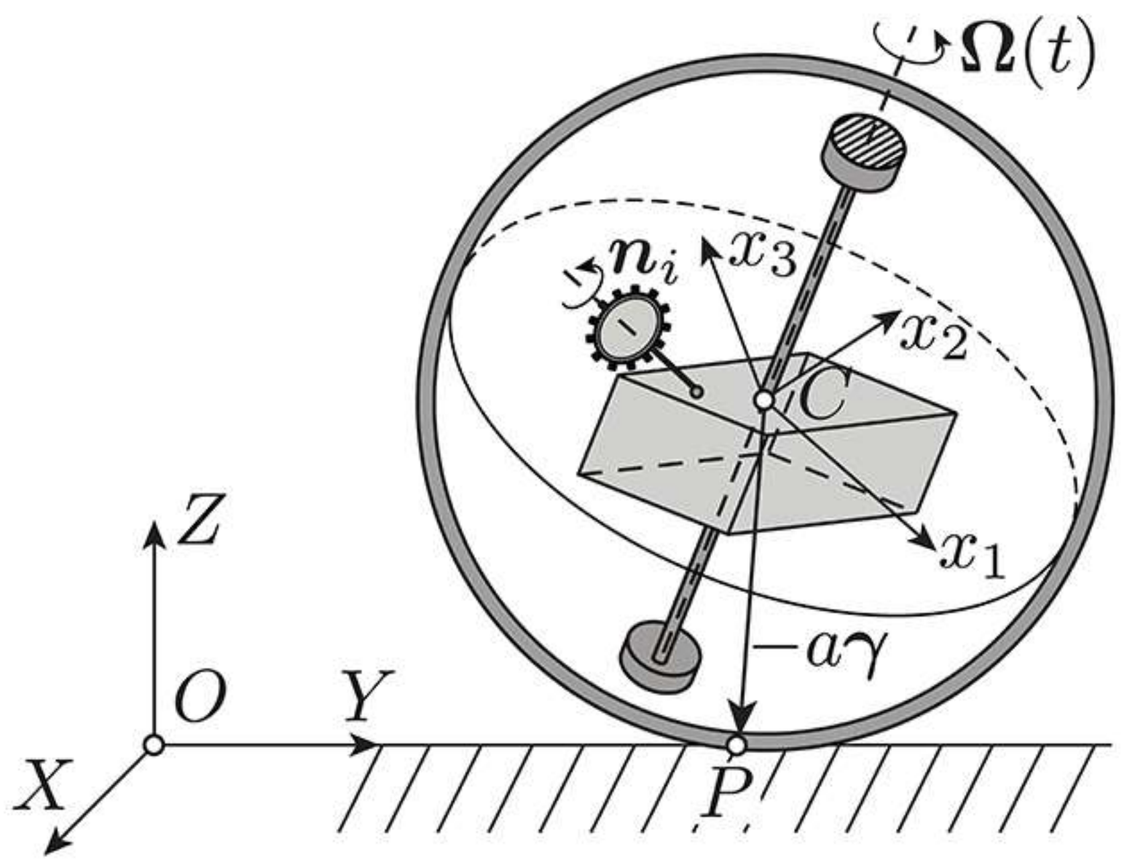

Fig. 4: The system on the plane.

A distinctive feature of this system is the fact that the mass distribution remains constant in the coordinate system $Cx_1x_2x_3$. This is due to the fact that the rotors and the shell in this system rotate in a prescribed manner about their symmetry axes (in contrast to the coordinate system attached to the shell).

Configuration space. Let $\boldsymbol{R}_C = (X_c, Y_c, Z_c)$ be the coordinates of the center of mass of the system in the inertial coordinate system $OXYZ$ and let $\mathbf{S}$ be the matrix of rotation of the fixed axes relative to the coordinate system attached to the frame $Cx_1x_2x_3$.

Let us parameterize $\mathbf{S}$ by $\boldsymbol{\alpha}$, $\boldsymbol{\beta}$ and $\boldsymbol{\gamma}$, the unit vectors of the inertial coordinate system referred to the axes $Cx_1x_2x_3$:

$$\mathbf{S} = \begin{pmatrix} \alpha_1 & \beta_1 & \gamma_1 \\ \alpha_2 & \beta_2 & \gamma_2 \\ \alpha_3 & \beta_3 & \gamma_3 \end{pmatrix} \in SO(3),$$

where the unit vector $\boldsymbol{\gamma}$ defines the normal to the plane, i.e., it is directed along the axis OZ.

REMARK 1. In this case, obvious geometric relations expressing the condition of orthogonality of the matrix $\mathbf{S}$ are satisfied:

$$(\boldsymbol{\alpha}, \boldsymbol{\beta}) = (\boldsymbol{\beta}, \boldsymbol{\gamma}) = (\boldsymbol{\gamma}, \boldsymbol{\alpha}) = 0,$$
$$\boldsymbol{\alpha}^2 = \boldsymbol{\beta}^2 = \boldsymbol{\gamma}^2 = 1.$$

Since the motion of the shell and the rotor relative to the frame is defined at any instant of time, the pair $\boldsymbol{R}_C$, $\boldsymbol{S}$ uniquely defines the configuration of the system. Thus,

$$\mathcal{N} = \{\boldsymbol{R}_C, \boldsymbol{S}\} \approx \mathbb{R}^3 \times SO(3)$$

is the configuration space of this system.

REMARK 2. Here and in what follows, we denote vectors by bold italic $\boldsymbol{a}, \boldsymbol{b}, \ldots$, and write their scalar and vector product as $(\boldsymbol{a}, \boldsymbol{b})$ and $\boldsymbol{a} \times \boldsymbol{b}$, respectively. The sign $\widehat{\ }$ above the vector denotes the skew-symmetric matrix $\widehat{\boldsymbol{a}} = \varepsilon_{ijk} a_k$, where ε_{ijk} is the Levi-Civita symbol. The sign $\otimes$ denotes a tensor product, i. e., in matrix form $\boldsymbol{a} \otimes \boldsymbol{b} = ||a_i b_j||$. Boldface upright font is used to denote the matrices: $\mathbf{A}, \mathbf{B}, \ldots$.

Quasi-velocities. We parameterize the tangent space $T\mathcal{N}$ by the velocity of the center of mass of the system, $\boldsymbol{v} = (v_1, v_2, v_3)$, and by the angular velocity of the frame, $\boldsymbol{\omega} = (\omega_1, \omega_2, \omega_3)$, which are referred to the moving axes $Cx_1x_2x_3$. They are expressed in terms of configuration variables and their derivatives as follows (see [17] for details):

$$\widehat{\boldsymbol{\omega}} = \dot{\mathbf{S}}\mathbf{S}^T, \quad \boldsymbol{v} = \mathbf{S}\dot{\boldsymbol{R}}_C,$$

$$\widehat{\boldsymbol{\omega}} = \begin{pmatrix} 0 & \omega_3 & -\omega_2 \\ -\omega_3 & 0 & \omega_1 \\ \omega_2 & -\omega_1 & 0 \end{pmatrix}.$$

Here and in what follows (unless otherwise specified), all vectors are referred to the moving axes $Cx_1x_2x_3$.

Models of rolling and constraint equations. Two nonholonomic models of a shell rolling on a plane are possible:

1. The model of rolling without slipping (*classical rolling model*), in which the velocity at the contact point of the shell is zero:

$$\boldsymbol{f} = \boldsymbol{v} + a\boldsymbol{\gamma} \times \big(\boldsymbol{\omega} - \boldsymbol{\Omega}(t)\big) = 0, \tag{1}$$

   where a is the radius of the spherical shell.

2. The model of rolling without slipping and spinning (*rubber rolling model*), which, in addition to assuming zero velocity of the point of contact, assumes that there is no spinning of the shell relative to $\boldsymbol{\gamma}$, the normal to the plane at the point of contact P:

$$f_0 = (\boldsymbol{\omega} - \boldsymbol{\Omega}(t), \boldsymbol{\gamma}) = 0. \tag{2}$$

   As a rule, this model is called the rubber rolling model [34, 27] to emphasize that, by coating the body with rubber, one can ensure a proper contact with the plane.

Thus, in the coordinate system $Cx_1x_2x_3$ nonholonomic constraints are given by relations that are inhomogeneous in the velocities $\boldsymbol{v}$ and $\boldsymbol{\omega}$.

Kinetic energy. The kinetic energy in the coordinate system $Cx_1x_2x_3$ can be represented as

$$T = \frac{1}{2}m\boldsymbol{v}^2 + \frac{1}{2}(\boldsymbol{\omega}, \mathbf{I}\boldsymbol{\omega}) + (\boldsymbol{k}(t), \boldsymbol{\omega}),$$

where m and $\mathbf{I}$ are, respectively, the mass and the tensor of inertia of the system, and $\boldsymbol{k}(t)$ is the vector of the total gyrostatic momentum of the rotors and the frame, which is expressed in terms of their angular velocities:

$$\boldsymbol{k}(t) = \sum_{i=1}^{n} j_i\dot{\phi}_i(t)\boldsymbol{n}_i - J_{\mathsf{s}}\boldsymbol{\Omega}(t),$$

where J_{s} and j_i are the moments of inertia of the shell and the ith rotor, respectively.

We direct the axes of the coordinate system $Cx_1x_2x_3$ along the principal axes of inertia of the system, thus, $\mathbf{I} = \operatorname{diag}(I_1, I_2, I_3)$ is a diagonal matrix.

Equations of motion. In the general case, we represent the equations of motion in the form of Poincaré – Suslov equations (for details, see [18, 38]):

$$\begin{gathered}\frac{d}{dt}\left(\frac{\partial T}{\partial \boldsymbol{\omega}}\right)+\boldsymbol{\omega}\times\frac{\partial T}{\partial \boldsymbol{\omega}}+\boldsymbol{v}\times\frac{\partial T}{\partial \boldsymbol{v}}+\boldsymbol{\gamma}\times\frac{\partial T}{\partial \boldsymbol{\gamma}}=\sum_{i=1}^{3}\lambda_i\frac{\partial f_i}{\partial \boldsymbol{\omega}}+\lambda_0\frac{\partial f_0}{\partial \boldsymbol{\omega}},\\ \frac{d}{dt}\left(\frac{\partial T}{\partial \boldsymbol{v}}\right)+\boldsymbol{\omega}\times\frac{\partial T}{\partial \boldsymbol{v}}=\sum_{i=1}^{3}\lambda_i\frac{\partial f_i}{\partial \boldsymbol{v}}+\lambda_0\frac{\partial f_0}{\partial \boldsymbol{v}},\end{gathered}\tag{3}$$

where $\boldsymbol{\lambda}=(\lambda_1,\lambda_2,\lambda_3)$ and λ_0 are the undetermined multipliers defining the reaction of the constraints (1) and (2), respectively.

REMARK 3. The center of mass of the entire system coincides with the geometric center, therefore, the system of equations (3) contains no terms with potential of the gravitational field (since $U=\mathrm{const}$).

Differentiating the constraint (1), we find from the last equation of (3):

$$\boldsymbol{\lambda}=-ma\boldsymbol{\gamma}\times\big(\dot{\boldsymbol{\omega}}-\dot{\boldsymbol{\Omega}}(t)\big)-ma\dot{\boldsymbol{\gamma}}\times\big(\boldsymbol{\omega}-\boldsymbol{\Omega}(t)\big)-ma\boldsymbol{\omega}\times\big(\boldsymbol{\gamma}\times(\boldsymbol{\omega}-\boldsymbol{\Omega}(t))\big).$$

Substituting $\boldsymbol{\lambda}$ thus found into the first equation of (3) and writing a kinematic relation for the normal vector $\boldsymbol{\gamma}$, we obtain

$$\begin{aligned}
\tilde{\mathbf{I}}\dot{\boldsymbol{\omega}} &= \big(\tilde{\mathbf{I}}\boldsymbol{\omega} + \boldsymbol{k}(t)\big) \times \boldsymbol{\omega} + ma^2\big(\boldsymbol{\omega} - \boldsymbol{\Omega}(t), \boldsymbol{\gamma}\big)\boldsymbol{\gamma} \times \boldsymbol{\omega} + \lambda_0\boldsymbol{\gamma} \\
&\quad + ma^2(\boldsymbol{\omega}, \boldsymbol{\gamma})\boldsymbol{\gamma} \times \boldsymbol{\Omega}(t) + ma^2\boldsymbol{\gamma} \times \big(\dot{\boldsymbol{\Omega}}(t) \times \boldsymbol{\gamma}\big) - \dot{\boldsymbol{k}}(t), \\
\tilde{\mathbf{I}} &= \mathbf{I} + ma^2(\boldsymbol{\gamma}^2 - \boldsymbol{\gamma} \otimes \boldsymbol{\gamma}), \\
\dot{\boldsymbol{\gamma}} &= \boldsymbol{\gamma} \times \boldsymbol{\omega}.
\end{aligned} \tag{4}$$

where $\tilde{\mathbf{I}}$ is the tensor of inertia of the system relative to the point of contact P.

In order to obtain equations of motion in the classical rolling model in the system (4)*, we need to set* $\lambda_0 = 0$*, and in the case of the rubber rolling model* λ_0 *is defined from the constraint* (2).

Differentiating the constraint (2) with respect to time, we obtain

$$(\tilde{\mathbf{I}}\dot{\boldsymbol{\omega}}, \tilde{\mathbf{I}}^{-1}\boldsymbol{\gamma}) - (\boldsymbol{\Omega}(t), \boldsymbol{\gamma} \times \boldsymbol{\omega}) + (\dot{\boldsymbol{\Omega}}(t), \boldsymbol{\gamma}) = 0.$$

From this equation, taking (4) into account, we find the undetermined multiplier λ_0 as a function of the angular velocity $\boldsymbol{\omega}$ and of the normal $\boldsymbol{\gamma}$:

$$\lambda_0 = -\frac{\left(\tilde{\mathbf{I}}^{-1}\boldsymbol{\gamma}, \left(\tilde{\mathbf{I}}\boldsymbol{\omega} + \boldsymbol{k}(t)\right) \times \boldsymbol{\omega} + ma^2\left(\boldsymbol{\omega} - \boldsymbol{\Omega}(t), \boldsymbol{\gamma}\right)\boldsymbol{\gamma} \times \boldsymbol{\omega} + \boldsymbol{W}\right)}{(\tilde{\mathbf{I}}^{-1}\boldsymbol{\gamma}, \boldsymbol{\gamma})} + \frac{(\boldsymbol{\Omega}(t), \boldsymbol{\gamma} \times \boldsymbol{\omega}) + (\dot{\boldsymbol{\Omega}}(t), \boldsymbol{\gamma})}{(\tilde{\mathbf{I}}^{-1}\boldsymbol{\gamma}, \boldsymbol{\gamma})}, \tag{5}$$

$$\boldsymbol{W} = ma^2(\boldsymbol{\omega}, \boldsymbol{\gamma})\boldsymbol{\gamma} \times \boldsymbol{\Omega}(t) + ma^2\boldsymbol{\gamma} \times \left(\dot{\boldsymbol{\Omega}}(t) \times \boldsymbol{\gamma}\right) - \dot{\boldsymbol{k}}(t).$$

We see that Eqs. (4) are closed relative to the variables $\boldsymbol{\omega}$, $\boldsymbol{\gamma}$ and form a reduced system.

Reconstruction of dynamics. From the known functions $\boldsymbol{\omega}(t)$ and $\boldsymbol{\gamma}(t)$ the orientation of the frame is described by the following system of equations:

$$\dot{\boldsymbol{\alpha}} = \boldsymbol{\alpha} \times \boldsymbol{\omega}, \quad \dot{\boldsymbol{\beta}} = \boldsymbol{\beta} \times \boldsymbol{\omega}. \tag{6}$$

The equations of motion for the coordinates of the contact point $\boldsymbol{R}_P = (X, Y, 0)$ of the shell in the fixed coordinate system $OXYZ$ have the form

$$\dot{X} = a\big(\boldsymbol{\beta}, \boldsymbol{\omega} - \boldsymbol{\Omega}(t)\big), \quad \dot{Y} = -a\big(\boldsymbol{\alpha}, \boldsymbol{\omega} - \boldsymbol{\Omega}(t)\big). \tag{7}$$

In the noninertial coordinate system $Cx_1x_2x_3$ (attached to the frame) the equations of motion (4), (6) and (7) have a simpler form than the equations in the coordinate system attached to the shell, which makes them amenable to a detailed qualitative analysis.

Below, we will consider separately the case of the rubber rolling and that of the classical rolling of the ball, since the conservation laws for them are different.

REMARK 4. In this case, the symmetry group of the entire system is the group of motions of the plane $SE(2)$. We see that the components of the vectors $\boldsymbol{\omega}$ and $\boldsymbol{\gamma}$ are its invariants. Consequently, choosing the suitable coordinate system $Cx_1x_2x_3$, we have in fact performed a reduction by symmetries.

3. CONSERVATION LAWS

3.1. Rolling of the Shell Without Slipping and Spinning (Rubber Model)

Let us define the angular momentum:

$$\boldsymbol{M} = \boldsymbol{\gamma} \times \left(\tilde{\mathbf{I}}\boldsymbol{\omega} - \boldsymbol{K}(t)\right), \quad \boldsymbol{K}(t) = \boldsymbol{k}(t) - ma^2\boldsymbol{\Omega}(t), \tag{8}$$

which lies in the horizontal plane OXY:

$$(\boldsymbol{M}, \boldsymbol{\gamma}) = 0.$$

The equations of motion for $\boldsymbol{M}$ and $\boldsymbol{\gamma}$, taking the constraint (2) into account, can be represented as

$$\dot{\boldsymbol{M}} = \boldsymbol{M} \times \boldsymbol{\omega}, \quad \dot{\boldsymbol{\gamma}} = \boldsymbol{\gamma} \times \boldsymbol{\omega},$$

$$\boldsymbol{\omega} = \mathbf{A}\left(\frac{\boldsymbol{M} \times \mathbf{A}\boldsymbol{\gamma}}{(\mathbf{A}\boldsymbol{\gamma}, \boldsymbol{\gamma})} - \boldsymbol{K}(t) + Z\boldsymbol{\gamma}\right), \quad Z = \frac{(\boldsymbol{\Omega}(t) + \mathbf{A}\boldsymbol{K}(t), \boldsymbol{\gamma})}{(\mathbf{A}\boldsymbol{\gamma}, \boldsymbol{\gamma})}, \tag{9}$$

where $\mathbf{A} = \operatorname{diag}(a_1, a_2, a_3) = (\mathbf{I} + ma^2\mathbf{E})^{-1}$ is the diagonal matrix.

As can be seen, the angular momentum $\boldsymbol{M}$ is constant in the fixed coordinate system $OXYZ$, and hence the reduced system (9) possesses the following integrals of motion:

$$F_0 = \boldsymbol{\gamma}^2, \quad F_1 = (\boldsymbol{M}, \boldsymbol{\gamma}), \quad F_2 = \boldsymbol{M}^2,$$

and, according to the definition of $\boldsymbol{M}$ and $\boldsymbol{\gamma}$, we obtain $F_0 = 1$, $F_1 = 0$.

Now suppose that the angular velocity of the frame and the generalized gyrostatic momentum *do not depend explicitly on time*:

$$\boldsymbol{\Omega} = \text{const}, \quad \boldsymbol{K} = \text{const}.$$

Then the problem reduces to investigating the autonomous system of Eqs. (9), which describes the flow on the three-dimensional manifold parameterized by the value of the integral $F_2 = f = \text{const}$:

$$\mathcal{M}^3_f = \{(\boldsymbol{M}, \boldsymbol{\gamma}) \mid \boldsymbol{\gamma}^2 = 1, (\boldsymbol{M}, \boldsymbol{\gamma}) = 0, \boldsymbol{M}^2 = f\},$$

which is a bundle of unit tangent vectors [40].

REMARK 5. If $\boldsymbol{\Omega} \neq 0$, then the nonholonomic constraints (1) and (2) are inhomogeneous in the velocities. As is well known [26, 35], the equations of motion (9) generally have no energy integral for such systems. Nevertheless, if $\mathbf{A}$ is an axisymmetric matrix and the vectors $\boldsymbol{\Omega}$ and $\boldsymbol{K}$ are directed along its symmetry axis, then the system (9) describes the rolling of a balanced *Routh sphere* with a rotor. In this case, the system (9) has an energy integral and an invariant measure (i. e., it is integrable by quadratures [45, 20]) in the rubber and the classical rolling model. We will not consider this case in what follows.

For the system (9) to be integrable by the Euler – Jacobi theorem, we need an additional integral and an invariant measure. Below it will be shown that in the general case the system (9) has chaotic trajectories, which suggests that it has no analytic integrals. In addition, simple and strange attractors will be found, and so, in the general case, there is no invariant measure with continuous density.

3.2. Rolling of the Shell Without Slipping (Classical Model) It turns out that, in the case of the classical rolling model there also exists angular momentum M, which is constant in the fixed coordinate system $OXYZ$. We represent it in the following form:

$$M = \tilde{\mathbf{I}}\boldsymbol{\omega} + \boldsymbol{K}(t) - d(\boldsymbol{\Omega}(t), \boldsymbol{\gamma})\boldsymbol{\gamma}, \quad \boldsymbol{K}(t) = \boldsymbol{k}(t) - d\boldsymbol{\Omega}(t), \ d = ma^2.$$

The reduced equations of motion for M and $\boldsymbol{\gamma}$ have the form

$$\dot{\boldsymbol{M}} = \boldsymbol{M} \times \boldsymbol{\omega}, \quad \dot{\boldsymbol{\gamma}} = \boldsymbol{\gamma} \times \boldsymbol{\omega},$$

$$\boldsymbol{\omega} = \mathbf{A}(\boldsymbol{M} - \boldsymbol{K}(t) + Z\boldsymbol{\gamma}), \quad Z = \frac{\big(\mathbf{A}(\boldsymbol{M} - \boldsymbol{K}(t)) - \boldsymbol{\Omega}, \boldsymbol{\gamma}\big)}{d^{-1} - (\mathbf{A}\boldsymbol{\gamma}, \boldsymbol{\gamma})}, \tag{10}$$

where $\mathbf{A} = (\mathbf{I} + ma^2\mathbf{E})^{-1}$ is the diagonal matrix.

Thus, the system possesses the following integrals of motion:

$$F_0 = \boldsymbol{\gamma}^2, \quad F_1 = (\boldsymbol{M}, \boldsymbol{\gamma}), \quad F_2 = \boldsymbol{M}^2,$$

where $F_0 = 1$ and, in contrast to the rubber model, in the general case one has $F_1 \neq 0$.

If one assumes the angular velocity of the frame and the gyrostatic momentum to be constant ($\boldsymbol{\Omega} = \text{const}$, $\boldsymbol{K} = \text{const}$), then, as in the rubber rolling model, the problem reduces to investigating the autonomous system of equations (9), which describes the flow on the three-dimensional manifold parameterized by the values of the integrals $F_1 = c = \text{const}$ and $F_2 = f = \text{const}$:

$$\mathcal{M}^3_{c,f} = \{(\boldsymbol{M}, \boldsymbol{\gamma}) \mid \boldsymbol{\gamma}^2 = 1, (\boldsymbol{M}, \boldsymbol{\gamma}) = c, \boldsymbol{M}^2 = f\}.$$

For the system (10) to be integrable by the Euler – Jacobi theorem, we need an additional integral and an invariant measure.

3.3. Reconstruction for Fixed Values of First Integrals

In this case, by choosing the orientation of the axes of the fixed coordinate system one can eliminate the equations of motion (6) for the unit vectors $\boldsymbol{\alpha}$ and $\boldsymbol{\beta}$ (i. e., perform reduction). We describe this procedure in more detail.

Let $\boldsymbol{M} \neq 0$ and $\boldsymbol{M} \nparallel \boldsymbol{\gamma}$ (the latter condition is automatically satisfied for the rubber rolling model, since $(\boldsymbol{M}, \boldsymbol{\gamma}) = 0$). Then on the fixed level set of the first integrals $\boldsymbol{M}^2 = f$, $(\boldsymbol{M}, \boldsymbol{\gamma}) = c$ we choose the unit vectors $\boldsymbol{\alpha}$ and $\boldsymbol{\beta}$ in the form

$$\boldsymbol{\alpha} = -\frac{\boldsymbol{M} - c\boldsymbol{\gamma}}{\sqrt{f - c^2}}, \quad \boldsymbol{\beta} = \frac{\boldsymbol{M} \times \boldsymbol{\gamma}}{\sqrt{f - c^2}}.$$

This yields equations for the trajectory of the point of contact in the form

$$\dot{X} = \frac{a}{\sqrt{f - c^2}}(\boldsymbol{M} \times \boldsymbol{\gamma}, \boldsymbol{\omega} - \boldsymbol{\Omega}), \quad \dot{Y} = \frac{a}{\sqrt{f - c^2}}(\boldsymbol{M} - c\boldsymbol{\gamma}, \boldsymbol{\omega} - \boldsymbol{\Omega}),$$

where $\boldsymbol{\omega}$ is expressed explicitly in terms of $\boldsymbol{M}$ and $\boldsymbol{\gamma}$ for the rubber rolling model from relation (9), and for the classical rolling model, from the formulae (10). For the rubber rolling model, in these relations we also need to set $c = 0$.

We note that in both cases (the rubber rolling model and the classical rolling model) preservation of the squared momentum $F_2 = M^2$ leads to boundedness of the trajectories of the reduced system (9). Thus, *there are no trajectories in which the shell accelerates constantly*. In addition, the existence of additional integrals allows one to reduce the problem to investigating a two-dimensional Poincaré map, to single out various partial solutions and to study them. Below we consider in more detail the rubber model of a rolling shell.

4. MOTION OF THE SYSTEM FROM REST FOR THE RUBBER MODEL OF A ROLLING SHELL

Consider the system (9) (i.e., the rubber rolling model) on the zero level set of the integral $F_2 = \boldsymbol{M}^2 = 0$ and at constant values $\boldsymbol{\Omega} = \text{const}$, $\boldsymbol{K} = \text{const}$. It follows from $F_2 = 0$ that each component of the vector of momentum $\boldsymbol{M} = 0$ is zero.

This case can be physically realized, for example, if one begins to increase the angular velocity of the frame $\boldsymbol{\Omega}(t)$ and the gyrostatic momentum $\boldsymbol{K}(t)$ from rest $(\boldsymbol{\omega} = \boldsymbol{\Omega} = \boldsymbol{K} = 0)$ to some fixed values $\boldsymbol{\Omega} = \text{const}$, $\boldsymbol{K} = \text{const}$. In this case, the value $\boldsymbol{M} = 0$ will remain unchanged, since $F_2 = \boldsymbol{M}^2$ is also a first integral if $\boldsymbol{\Omega}(t)$ and $\boldsymbol{K}(t)$ depend explicitly on time.

In this case the reduced system describes a vector field on a two-dimensional sphere:

$$\mathcal{M}_0^2 = \{(\boldsymbol{M}, \boldsymbol{\gamma}) \mid \boldsymbol{M} = 0, \boldsymbol{\gamma}^2 = 1\} \approx \mathbb{S}^2,$$

which has the form

$$\dot{\boldsymbol{\gamma}} = \boldsymbol{\gamma} \times \mathbf{A}\,(Z\boldsymbol{\gamma} - \boldsymbol{K}), \quad Z = \frac{(\boldsymbol{\Omega} + \mathbf{A}\boldsymbol{K}, \boldsymbol{\gamma})}{(\mathbf{A}\boldsymbol{\gamma}, \boldsymbol{\gamma})}. \tag{11}$$

The remaining equations of motion for defining the orientation of the frame and the trajectory of the point of contact can be represented as

$$\begin{gathered} \dot{\boldsymbol{\alpha}} = \boldsymbol{\alpha} \times \mathbf{A}\,(Z\boldsymbol{\gamma} - \boldsymbol{K}), \quad \dot{\boldsymbol{\beta}} = \boldsymbol{\beta} \times \mathbf{A}\,(Z\boldsymbol{\gamma} - \boldsymbol{K}), \\ \dot{X} = a\big(\boldsymbol{\beta}, \mathbf{A}\,(Z\boldsymbol{\gamma} - \boldsymbol{K}) - \boldsymbol{\Omega}\big), \quad \dot{Y} = -a\big(\boldsymbol{\alpha}, \mathbf{A}\,(Z\boldsymbol{\gamma} - \boldsymbol{K}) - \boldsymbol{\Omega}\big). \end{gathered} \tag{12}$$

Thus, at the first stage the problem reduces to investigating the two-dimensional autonomous system (11), in which chaotic trajectories are known to be absent.

When $\boldsymbol{\Omega} = 0$, the system (11) describes a particular case of generalization of the problem of the rubber Chaplygin ball with a gyrostat [8, 27] and admits the first integral

$$\frac{(\mathbf{A}\boldsymbol{K}, \boldsymbol{\gamma})^2}{(\mathbf{A}\boldsymbol{\gamma}, \boldsymbol{\gamma})} = \text{const}.$$

In the general case, the level surface of this integral is an elliptic cone, so that in this case all trajectories of the system (11) on the sphere $\boldsymbol{\gamma}^2 = 1$ turn out to be closed. Below it will be shown that, if $\boldsymbol{\Omega} \neq 0$, then the system (11) has asymptotically stable equilibrium points and limit cycles.

REMARK 6. The system (11) possesses the symmetry $\boldsymbol{\gamma} \to -\boldsymbol{\gamma}$. As a result, isolated fixed points occur in pairs.

5. REGULAR AND CHAOTIC MOTIONS FOR THE RUBBER MODEL OF A ROLLING SHELL

5.1. Straight-line Motions The reduced system (9) possesses a degenerate one-parameter family of the simplest equilibrium points for which $\boldsymbol{\omega} = 0$:

$$\Sigma^1 = \left\{ \boldsymbol{M} = \boldsymbol{\gamma}_0 \times \boldsymbol{K},\ \boldsymbol{\gamma} = \boldsymbol{\gamma}_0 \mid (\boldsymbol{\Omega}, \boldsymbol{\gamma}_0) = 0,\ \boldsymbol{\gamma}_0^2 = 1 \right\},\ \boldsymbol{\gamma}_0 = \text{const}. \tag{17}$$

In this case, the frame is at rest relative to the fixed coordinate system $OXYZ$, and the contact point P of the spherical shell traces out a straight line on the plane OXY.

REMARK 8. From the viewpoint of technical and engineering applications, these solutions are of particularly great importance, since it is in this case that the stabilization of the frame (and the devices connected with it) relative to the fixed coordinate system is achieved. A similar method of gyroscopic stabilization is used in a segway, which is a frame connected with a wheel pair (instead of a spherical shell).

Let us analyze the stability of the found solutions. The characteristic polynomial of the linearized system (9) in a neighborhood of the equilibrium points Σ^1 is represented as

$$P(\lambda) = \lambda^3 P_3(\lambda),$$

$$P_3(\lambda) = \lambda^3 + \frac{(\mathbf{A}\boldsymbol{\gamma}_0, \boldsymbol{\gamma}_0 \times \boldsymbol{\Omega})}{(\mathbf{A}\boldsymbol{\gamma}_0, \boldsymbol{\gamma}_0)}\lambda^2 + \frac{\det \mathbf{A}}{(\mathbf{A}\boldsymbol{\gamma}_0, \boldsymbol{\gamma}_0)}\left((\boldsymbol{K}, \boldsymbol{\gamma}_0)^2 - (\boldsymbol{K}, \mathbf{A}^{-1}\boldsymbol{\Omega})\right)\lambda + \frac{\det \mathbf{A}}{(\mathbf{A}\boldsymbol{\gamma}_0, \boldsymbol{\gamma}_0)}(\boldsymbol{K}, \boldsymbol{\gamma}_0)(\boldsymbol{K}, \boldsymbol{\gamma}_0 \times \boldsymbol{\Omega}). \tag{18}$$

We see that the last term in $P_3(\lambda)$ vanishes for $\boldsymbol{K} = c\boldsymbol{\Omega}$, where $c = \mathrm{const}$ (i.e., $\boldsymbol{K} \parallel \boldsymbol{\Omega}$). In this case, the family Σ^1 lies entirely on the fixed level set of the integral $\mathcal{M}^3_f$, $f = \boldsymbol{K}^2$. In this case, the characteristic polynomial (18) has the form

$$P(\lambda) = \lambda^4 P_2(\lambda),$$

$$P_2(\lambda) = \lambda^2 + \frac{(\mathbf{A}\boldsymbol{\gamma}_0, \boldsymbol{\gamma}_0 \times \boldsymbol{\Omega})}{(\mathbf{A}\boldsymbol{\gamma}_0, \boldsymbol{\gamma}_0)}\lambda - \frac{\det \mathbf{A}}{(\mathbf{A}\boldsymbol{\gamma}_0, \boldsymbol{\gamma}_0)}(\boldsymbol{K}, \mathbf{A}^{-1}\boldsymbol{\Omega}).$$

In the general case ($\boldsymbol{K} \nparallel \boldsymbol{\Omega}$), the family Σ^1 is transverse to the level surfaces of the integrals $\mathcal{M}^3_f$. Thus, the fixed points from Σ^1 turn out to be isolated on $\mathcal{M}^3_f$. Next, we consider in detail only the case $\boldsymbol{K} \perp \boldsymbol{\Omega}$, since calculations simplify considerably in this case. A detailed analysis of all possible cases requires a separate study.

The case $\boldsymbol{K} \perp \boldsymbol{\Omega}$. The normal vector for the equilibrium points Σ^1 can be represented as

$$\boldsymbol{\gamma}_0 = c_1\boldsymbol{K} + c_2\boldsymbol{K} \times \boldsymbol{\Omega}. \tag{19}$$

Next, from the geometric integral and the integral $F_2 = f$ we find (taking $(\boldsymbol{\Omega}, \boldsymbol{K}) = 0$ into account):

$$\boldsymbol{K}^2(c_1^2 + c_2^2\boldsymbol{\Omega}^2) = 1,\ c_2^2\boldsymbol{K}^4\boldsymbol{\Omega}^2 = f.$$

Solving this system for the coefficients c_1 and c_2, we obtain

Proposition 3. *If $f < \boldsymbol{K}^2$, then on each level surface of the first integrals $\mathcal{M}^3_f$ there are four isolated equilibrium points Σ^1:*

$$\mathcal{M}^3_f \cap \Sigma^1 = \{\sigma_+ \cup \sigma_- \cup \delta_+ \cup \delta_-\},$$

$$\sigma_\pm = \left\{ c_1 = \pm\frac{\sqrt{\boldsymbol{K}^2 - f}}{\boldsymbol{K}^2},\ c_2 = \frac{\sqrt{f}}{\boldsymbol{K}^2\sqrt{\boldsymbol{\Omega}^2}} \right\},$$

$$\delta_\pm = \left\{ c_1 = \pm\frac{\sqrt{\boldsymbol{K}^2 - f}}{\boldsymbol{K}^2},\ c_2 = -\frac{\sqrt{f}}{\boldsymbol{K}^2\sqrt{\boldsymbol{\Omega}^2}} \right\}.$$

When $f = \boldsymbol{K}^2$, there are two of these equilibrium points and the family Σ^1 touches $\mathcal{M}^3_f$.

According to the Routh – Hurwitz criterion, for an equilibrium point to be stable, it is necessary that the free coefficient in the polynomial $P_3(\lambda)$ be positive. In this case, after substituting (19) into the characteristic polynomial (18) and after abbreviating the positive polynomial, we find the stability condition:

$$c_1 c_2 < 0.$$

This yields the following proposition.

Proposition 4. *On the fixed level set of the integrals $\mathcal{M}_f^3$, $f < \boldsymbol{K}^2$ the equilibrium points σ_+ and δ_- are unstable regardless of the parameters.*

Further, using the Routh – Hurwitz criterion, we find that, for σ_- and δ_+ to be stable, the following inequalities must be satisfied:

$$\Big(c_1\mathbf{A}\boldsymbol{K} + c_2\mathbf{A}(\boldsymbol{K}\times\boldsymbol{\Omega}), c_1\boldsymbol{\Omega}\times\boldsymbol{K} + c_2\boldsymbol{\Omega}^2\Big) > 0,$$

$$\Big(c_1\mathbf{A}\boldsymbol{K} + c_2\mathbf{A}(\boldsymbol{K}\times\boldsymbol{\Omega}), c_1\boldsymbol{\Omega}\times\boldsymbol{K} + c_2\boldsymbol{\Omega}^2\Big)\Big(c_1\boldsymbol{K}^4 - (\boldsymbol{K}, \mathbf{A}^{-1}\boldsymbol{\Omega})\Big) \qquad (20)$$

$$+c_1c_2\boldsymbol{K}^2\Big(c_1\mathbf{A}\boldsymbol{K} + c_2\mathbf{A}(\boldsymbol{K}\times\boldsymbol{\Omega}), (c_1\boldsymbol{K} + c_2\boldsymbol{K}\times\boldsymbol{\Omega})\Big)\boldsymbol{K}^2\boldsymbol{\Omega}^2 > 0.$$

A typical view of a stability region on the parameter plane (K_1, K_2) is shown in Fig. 9.

Numerical experiments (see Fig. 10) show that, if we choose parameters in the stability region in Fig. 9, then there exist trajectories which from the neighborhood of the unstable equilibrium point (σ_+ or δ_-) tend asymptotically to another equilibrium point (σ_- or δ_+).

The trajectory of the contact point for the equilibrium points $\sigma_\pm$ and $\delta_\pm$ is described by the relations

$$X(t) = x_0, \quad Y(t) = \pm a\sqrt{\mathbf{\Omega}^2}t + y_0,$$
$$x_0, y_0 = \text{const},$$

where the signs $+$ and $-$ correspond, respectively, to $\sigma_\pm$ and $\delta_\pm$. Thus, the shell rolls along a straight line parallel to the axis OY.

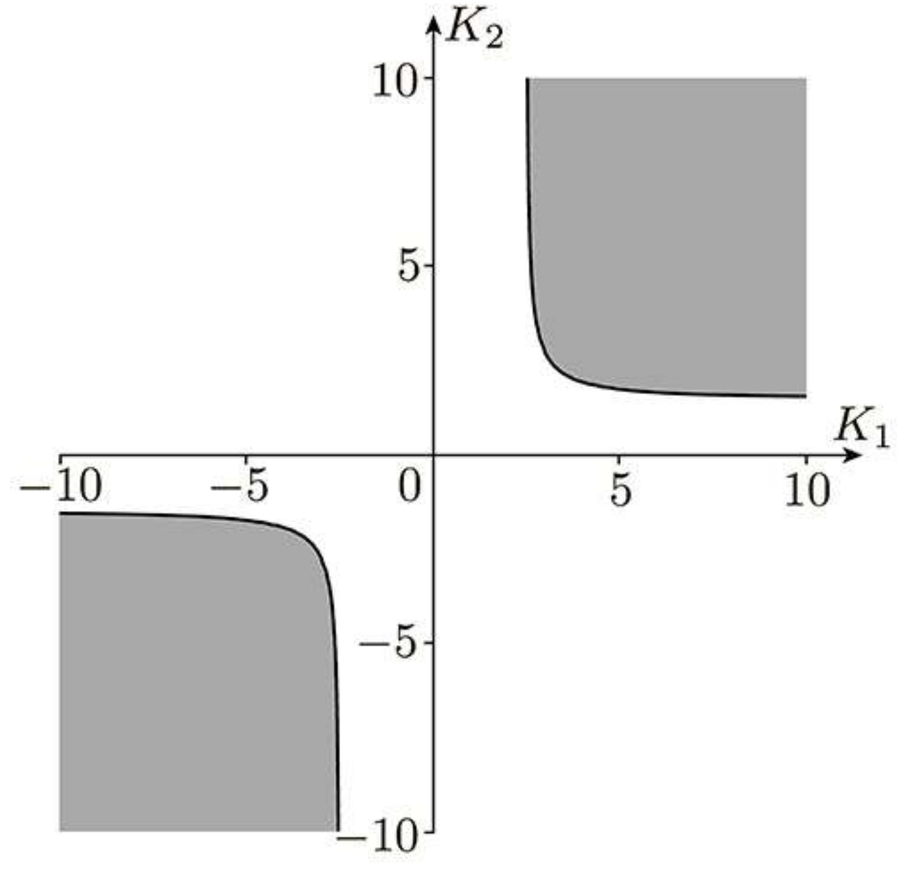

Fig. 9: The stability region (gray) of the equilibrium points σ_- and δ_+ on the parameter plane (K_1, K_2) for fixed $K_3 = 0$, $\mathbf{\Omega} = (0, 0, 1)$, $\mathbf{A} = \text{diag}(0.5, 0.3, 0.6)$.

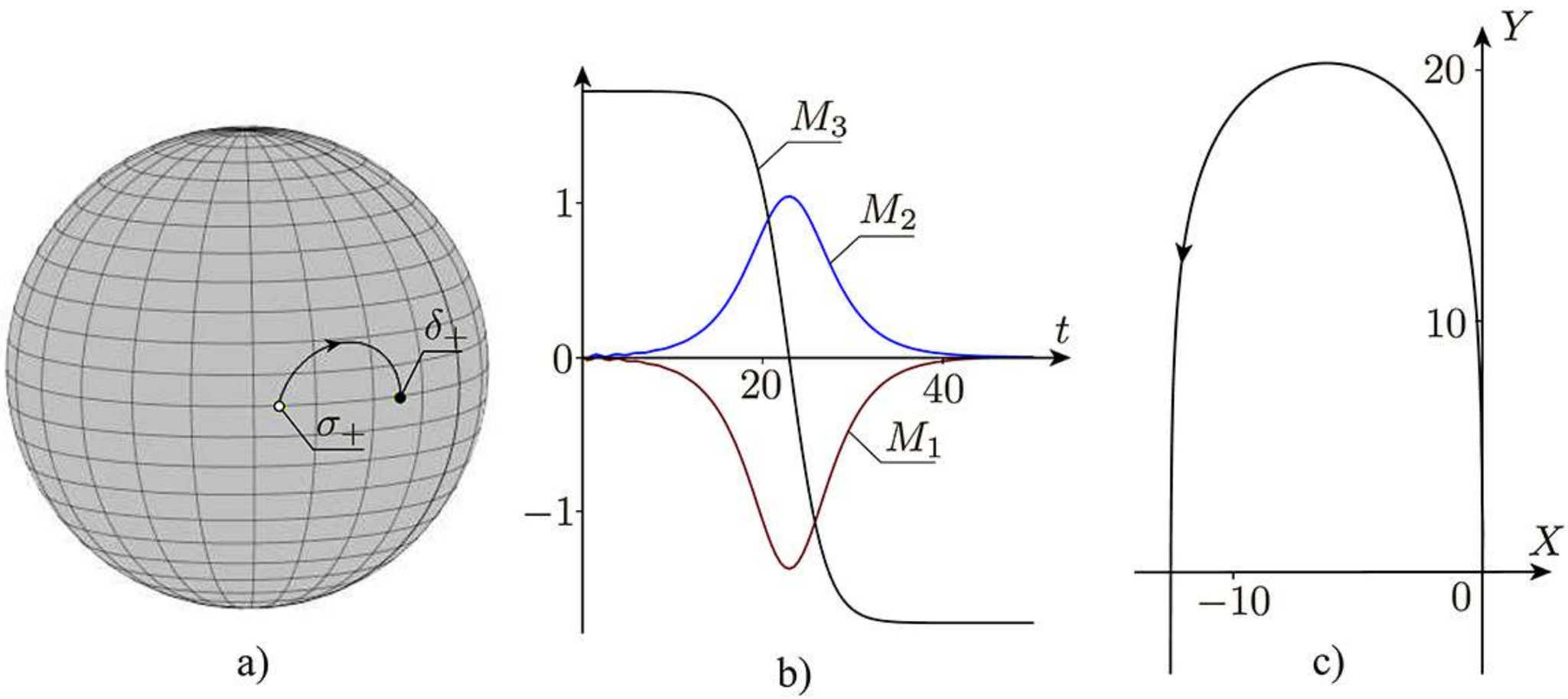

Fig. 10: Projection of the trajectory onto the Poisson sphere, the time dependence of the components of momentum $\boldsymbol{M}(t)$ and the trajectory of the contact point of the shell with the initial conditions from the neighborhood of the unstable equilibrium point σ_+ and $x(0) = 0$, $y(0) = 0$ for the fixed parameters: $\boldsymbol{\Omega} = (0, 0, 1)$, $\boldsymbol{K} = (4, 5, 0)$, $\mathbf{A} = \mathrm{diag}(0.5, 0.3, 0.6)$, $a = 1$, $f = 3$.

5.2. Restriction of the Flow to $\mathcal{M}^3_f$ and a Poincaré Map

To carry out a numerical analysis of the behavior of the trajectories of the reduced system (9) in the general case, in the absence of equilibrium points Σ^1 on the integral surfaces $\mathcal{M}^3_f$ (i. e., $f > \boldsymbol{K}^2$), we use a Poincaré map.

We first restrict this system to the three-dimensional manifold of the level set of the common integrals $\mathcal{M}^3_f$. For this, we use the Andoyer – Deprit variables (L, l, g) [17]:

$$M_1 = \sqrt{f - L^2}\sin l, \quad M_2 = \sqrt{f - L^2}\cos l, \quad M_3 = L,$$
$$\gamma_1 = \frac{L}{\sqrt{f}}\cos g \sin l + \sin g \cos l, \quad \gamma_2 = \frac{L}{\sqrt{f}}\cos g \cos l - \sin g \sin l, \tag{21}$$
$$\gamma_3 = -\sqrt{1 - \frac{L^2}{f}}\cos g,$$

where $l, g \in [0, 2\pi)$ are the angle variables and L, f satisfy the obvious inequality

$$-1 \leqslant \frac{L}{\sqrt{f}} \leqslant 1.$$

As a secant for this flow on $\mathcal{M}^3_f$ we choose the submanifold given by

$$g = g_0.$$

Numerically integrating the systems under consideration and finding the intersections of trajectories with the given section, we finally obtain a family of point two-dimensional maps:

$$\begin{gathered}\Phi_{f,g_0} : \mathcal{M}^2_{g_0} \to \mathcal{M}^2_{g_0}, \\ \mathcal{M}^2_{g_0} = \{\boldsymbol{x} \in \mathcal{M}^3 \mid g(\boldsymbol{x}) = g_0\}.\end{gathered} \tag{22}$$

We will parameterize the manifold $\mathcal{M}^2_{g_0}$ by a pair of variables $l \bmod 2\pi$ and $\frac{L}{\sqrt{f}}$ $\left(\left|\frac{L}{\sqrt{f}}\right| \leqslant 1\right)$ so that the pair $\left(l, \frac{L}{\sqrt{f}}\right)$ defines a point on the two-dimensional unit sphere S^2. The trajectories of this map for $g_0 = 0$ and different parameter values are shown in Fig. 11.

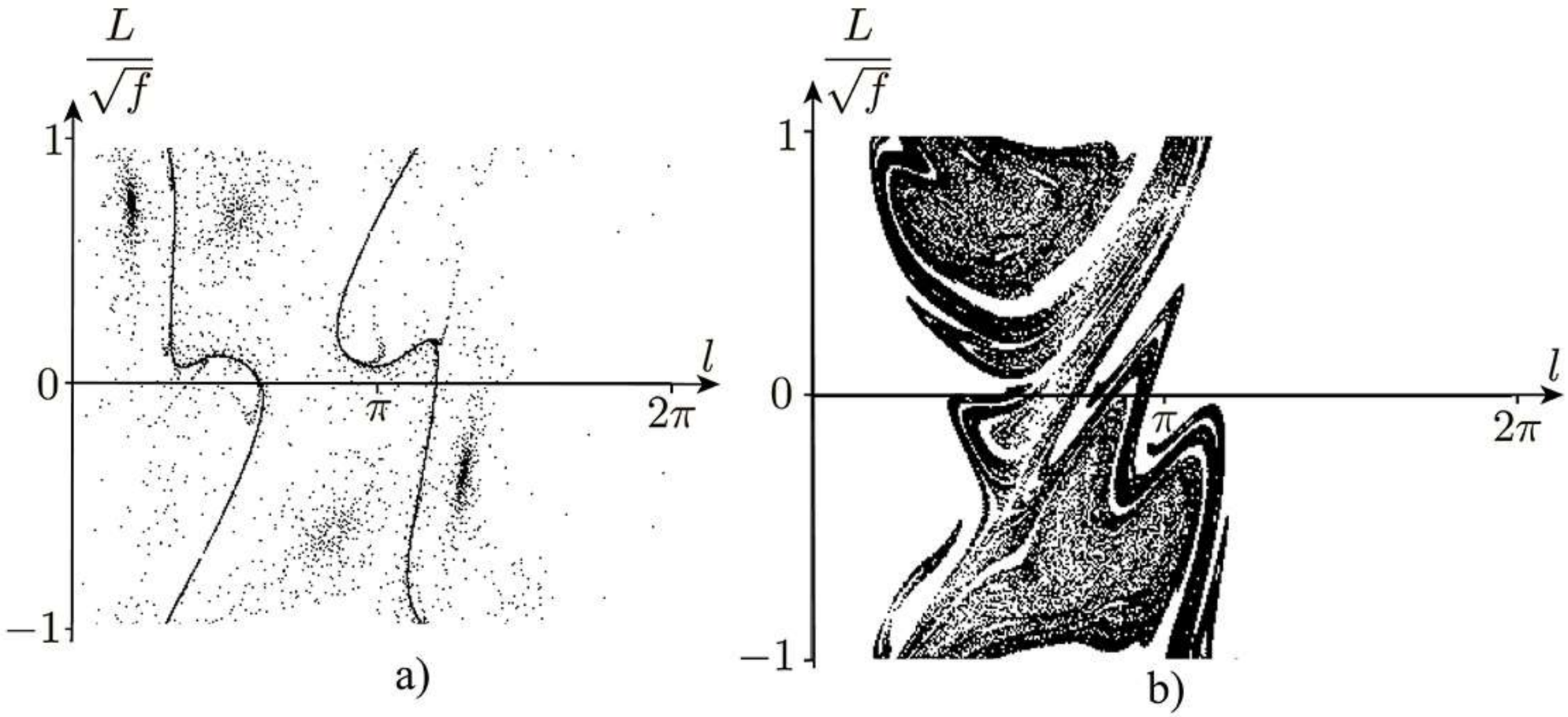

Fig. 11: A Poincaré map for the fixed parameters: a) $\boldsymbol{\Omega} = (0, 0, 2)$, $\boldsymbol{K} = (2, 2, 0)$, $\mathbf{A} = \mathrm{diag}(0.7, 0.6, 0.8)$, $f = 25$, b) $\boldsymbol{\Omega} = (0, 0, 2)$, $\boldsymbol{K} = (2, 3, 0)$, $\mathbf{A} = \mathrm{diag}(0.8, 0.6, 0.7)$, $f = 25$, $g_0 = 0$.

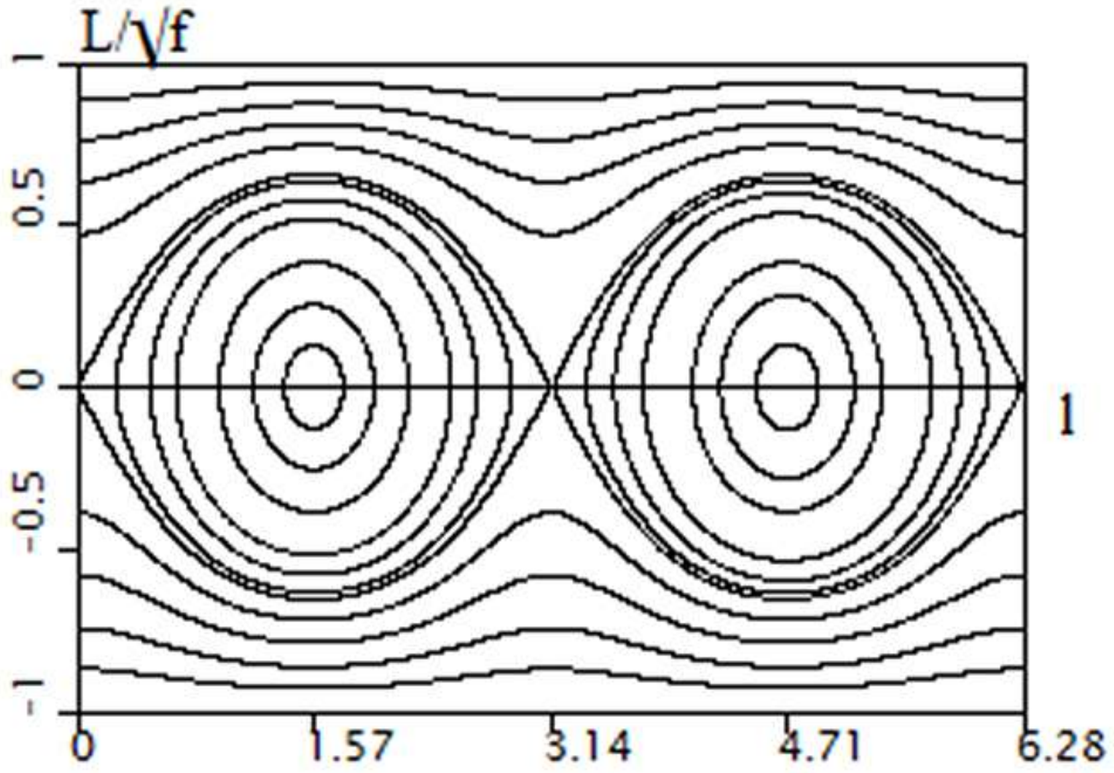

Fig. 12

l=diag (0.8, 0.7, 0,6), K=(0, 0, 0), Ω =(3, 2, 0), d=0, f=25, g_o=0

Fig. 13

l=diag (0.8, 0.7, 0,6), K=(0, 0, 0), Ω =(3, 2, 0), d=0.05, f=25, g_o=0

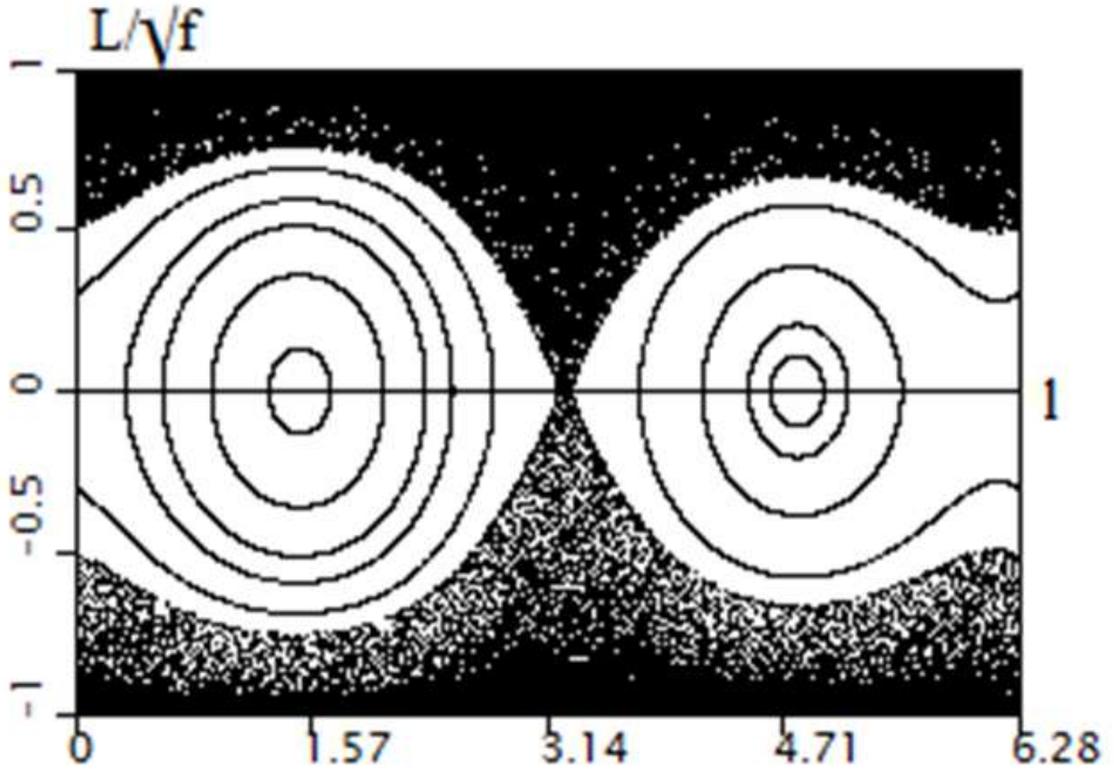

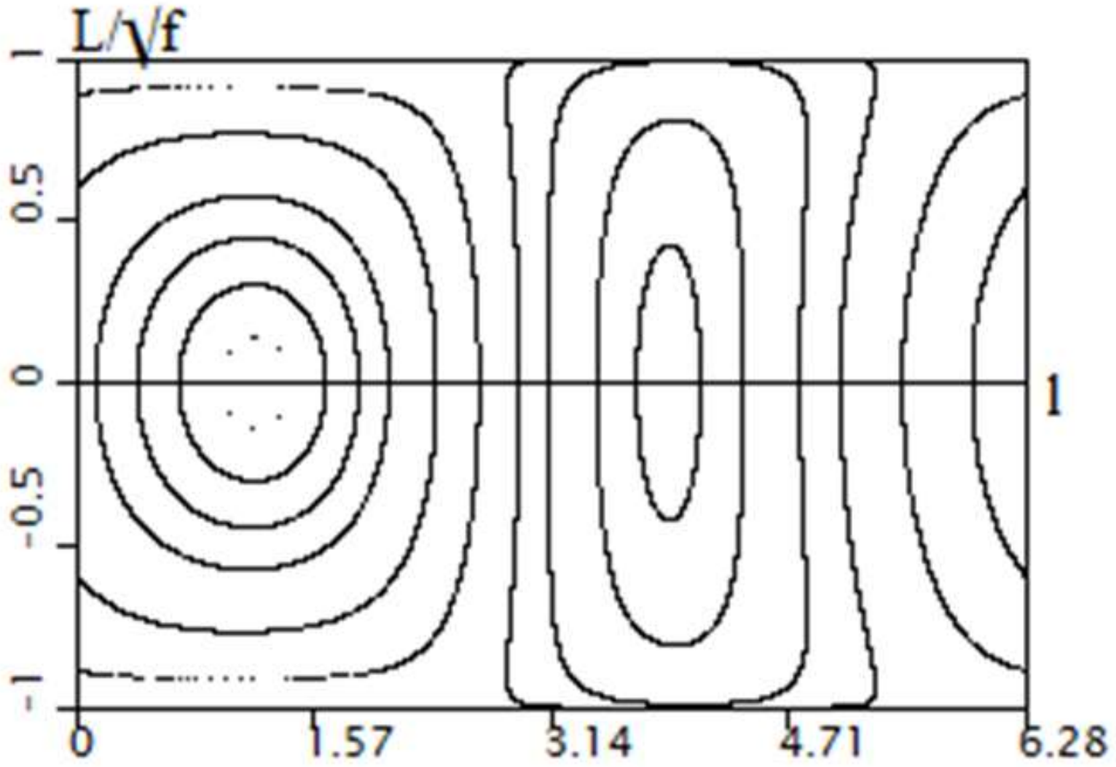

Fig. 14

l=diag (0.8, 0.7, 0,6), K=(0, 0, 0), Ω =(3, 2, 0),
d=0.4, f=25, g_o=0

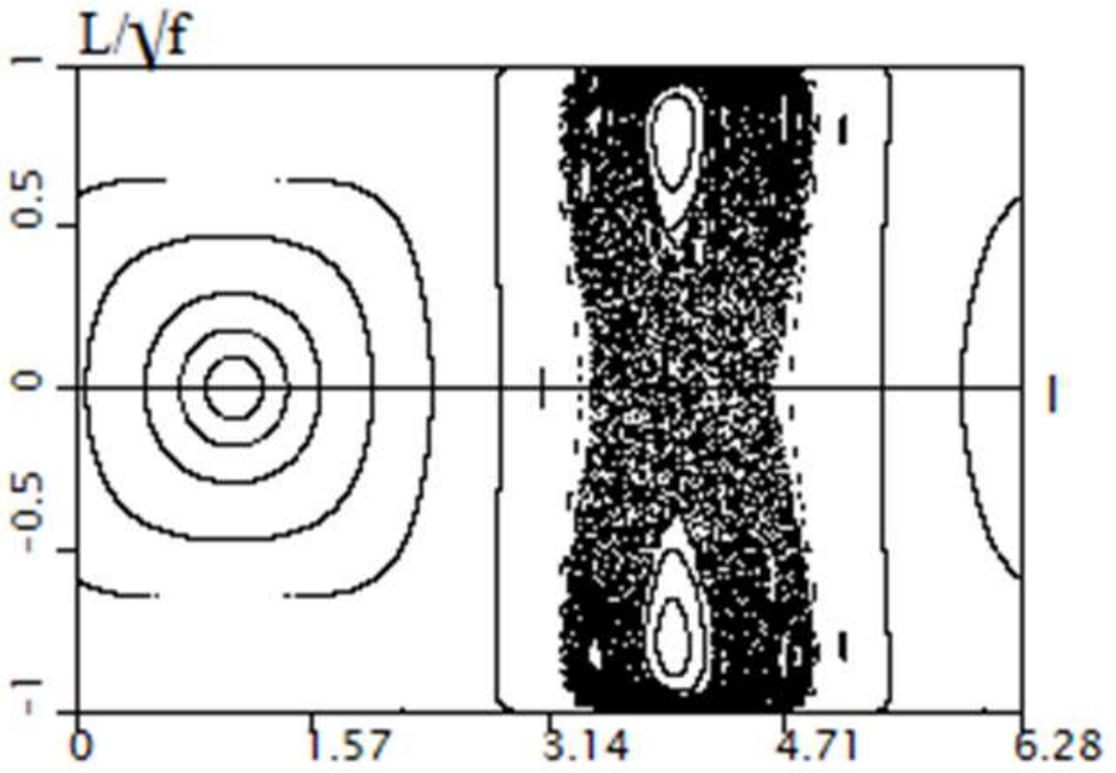

Fig. 15

l=diag (0.8, 0.7, 0,6), K=(0, 0, 0), Ω =(3, 2, 0),
d=1, f=25, g_o=0

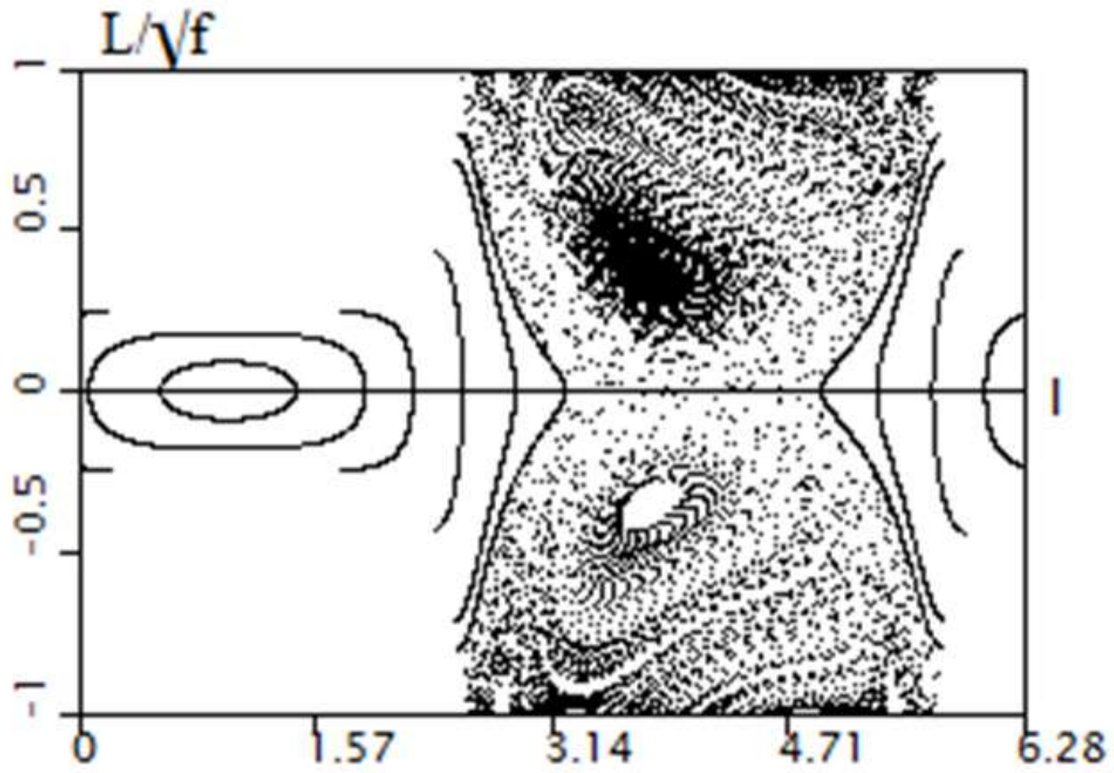

Fig. 16a

l=diag (0.8, 0.7, 0,6), K=(0, 0, 0), Ω =(3, 2, 0), d=4, f=25, g_0=0

Fig. 16b

The increase Poincare map

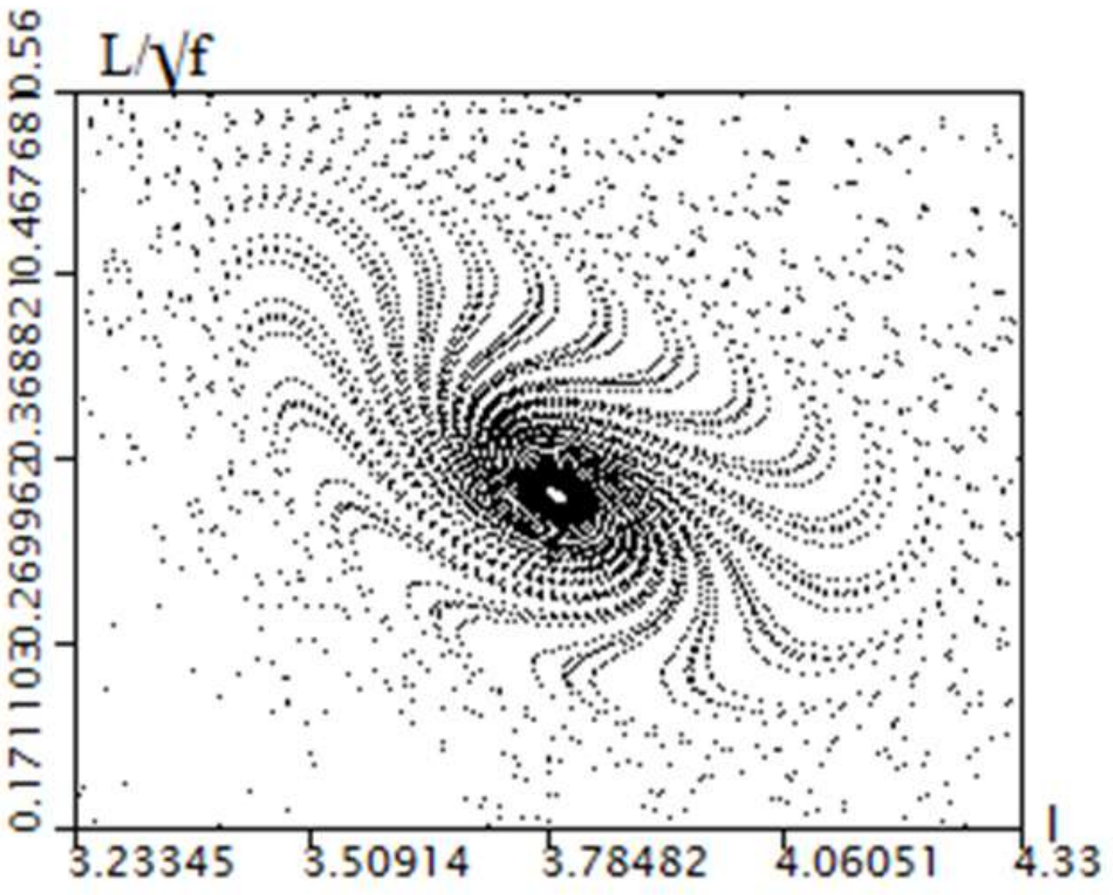

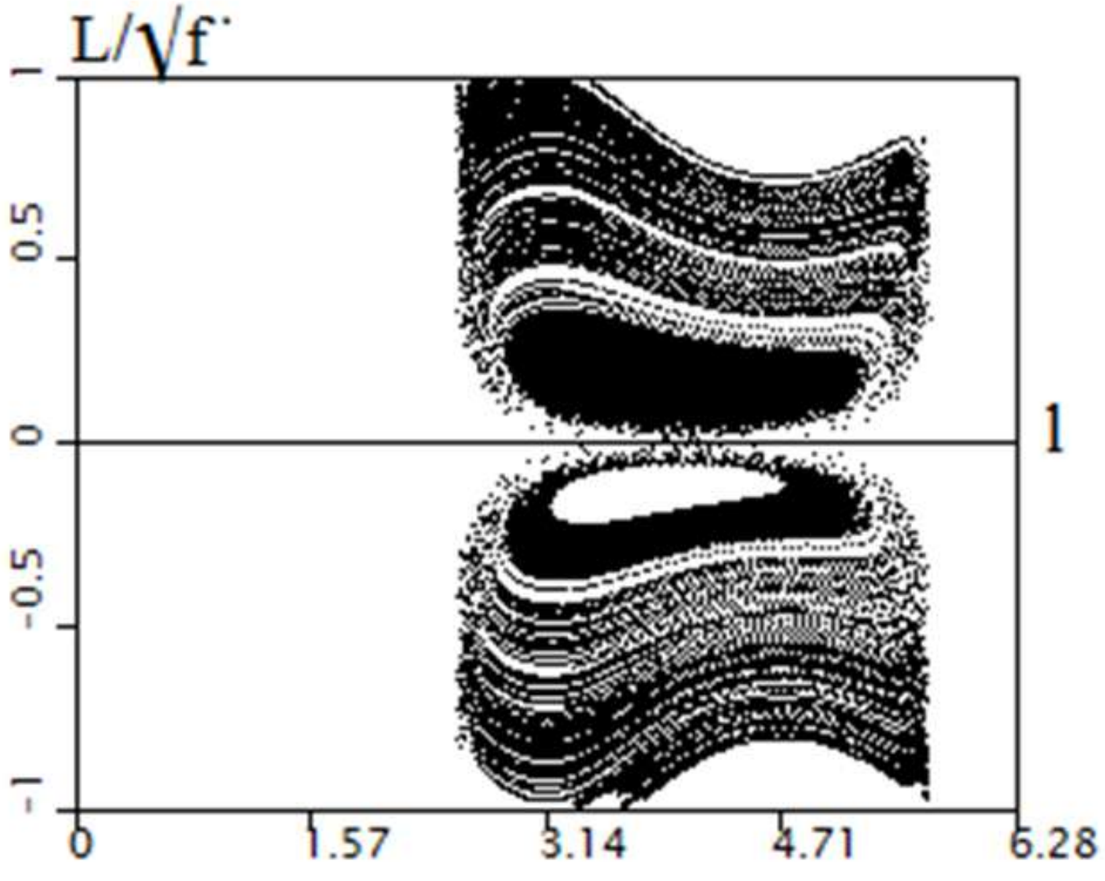

Fig. 17a

l=diag (0.8, 0.7, 0,6), K=(0, 0, 0), Ω =(3, 2, 0), d=20, f=25, g_0=0

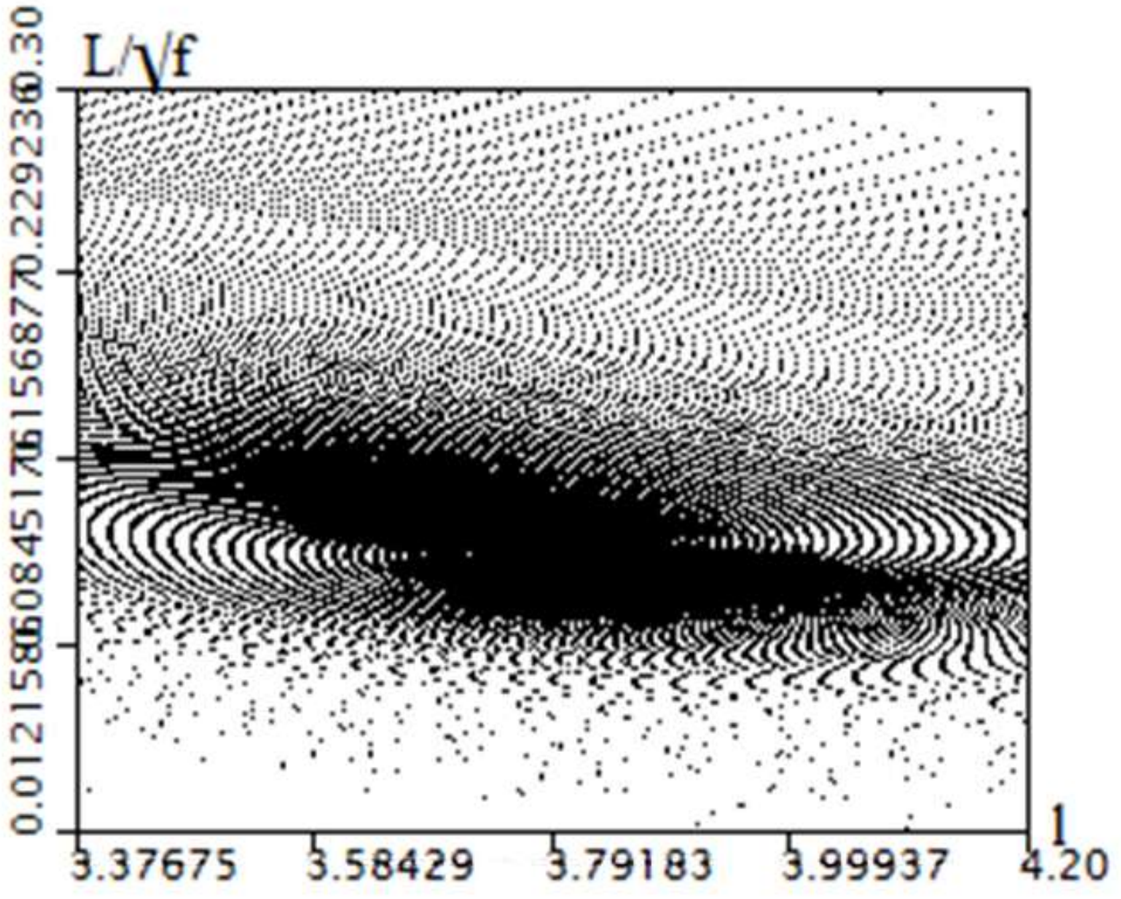

Fig. 17b

The increase Poincare map

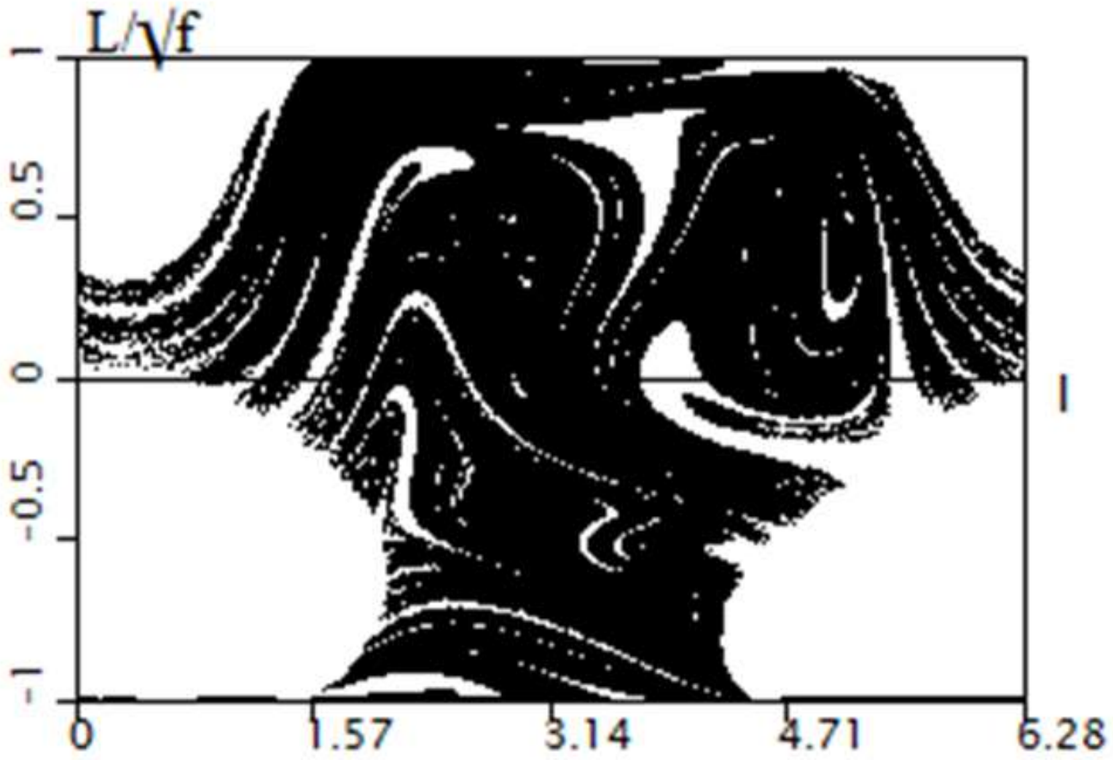

Fig. 18

l=diag (0.2, 0.5, 0,8), K=(2, 5, 4), Ω =(-2, 0, 2),
d=1.3, f=25, g_o=0

Fig. 19

l=diag (0.3, 0.5, 0,8), K=(2, 4, 0), Ω =(-2, 0, 2),
d=1.2, f=25, g_o=0

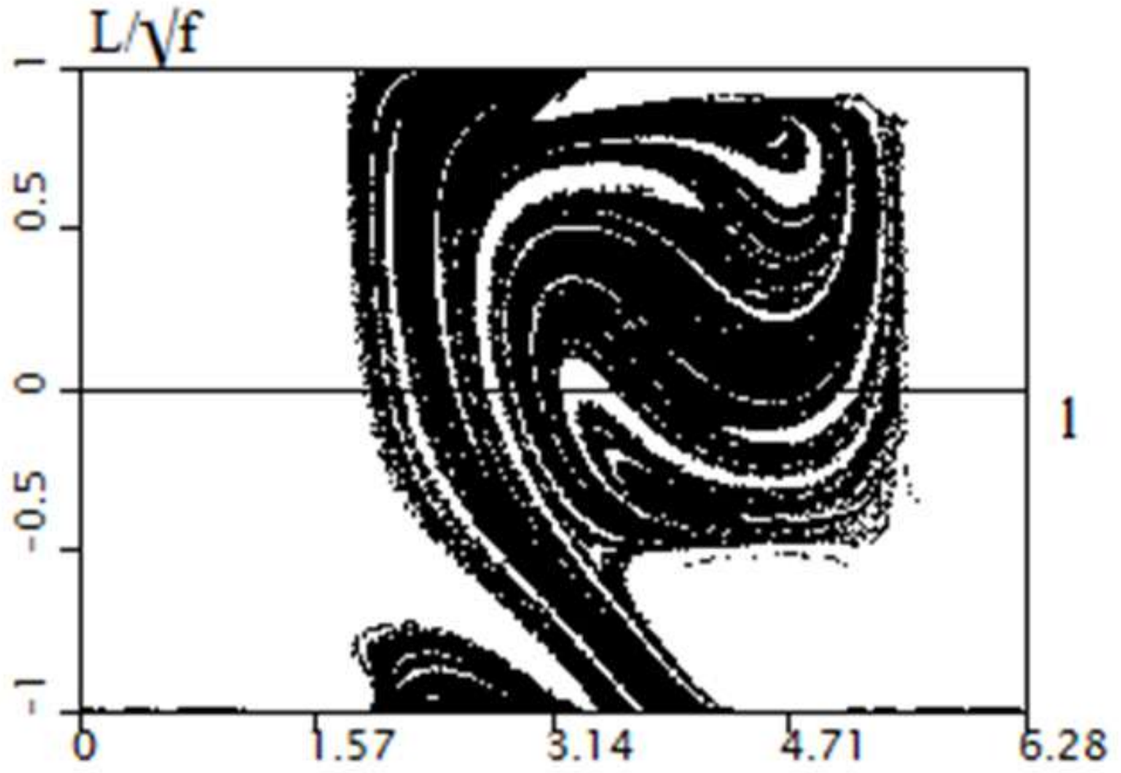

5.3. Asymptotically Stable Regimes of Motion (Attractors)

The numerical investigation of the Poincaré map has shown that the following types of attractors occur on it: fixed points, limit cycles and a strange (chaotic) attractor. In Fig. 11a, the fixed points Φ_{f,g_0} correspond to the largest concentration of points (almost black regions), and the limit cycle corresponds to the curve which on this involute of the sphere consists of two parts.

In $\mathcal{M}_f^3$, the fixed points of the map Φ_{f,g_0} correspond to a periodic solution and the invariant curve in Fig. 11a corresponds to a limit torus. The motion of the point of contact in this case is shown in Fig. 20b and Fig. 21b. The point of contact of the shell can be seen to undergo mean motion along the axis OX. Note that the displacement along the axis OY does not exceed some fixed value.

Moreover, a strange attractor arises at some parameters of the map Φ_{f,g_0} (see Fig. 11b). This attractor corresponds to the following Lyapunov exponents:

$$\Lambda_1 \approx 0.11, \quad \Lambda_2 \approx 0, \quad \Lambda_3 \approx 0, \quad \Lambda_4 \approx 0, \quad \Lambda_5 \approx 0, \quad \Lambda_6 \approx -0.13.$$

Its Kaplan – Yorke dimension on the Poincaré map is

$$D = 1 + \frac{\Lambda_1}{|\Lambda_6|} \approx 1.84.$$

The trajectory of the contact point for this case is shown in Fig. 22. As can be seen, the point of contact of the shell undergoes, as before, mean motion along the axis OX, but the deviation along the axis OY can increase (irregularly).

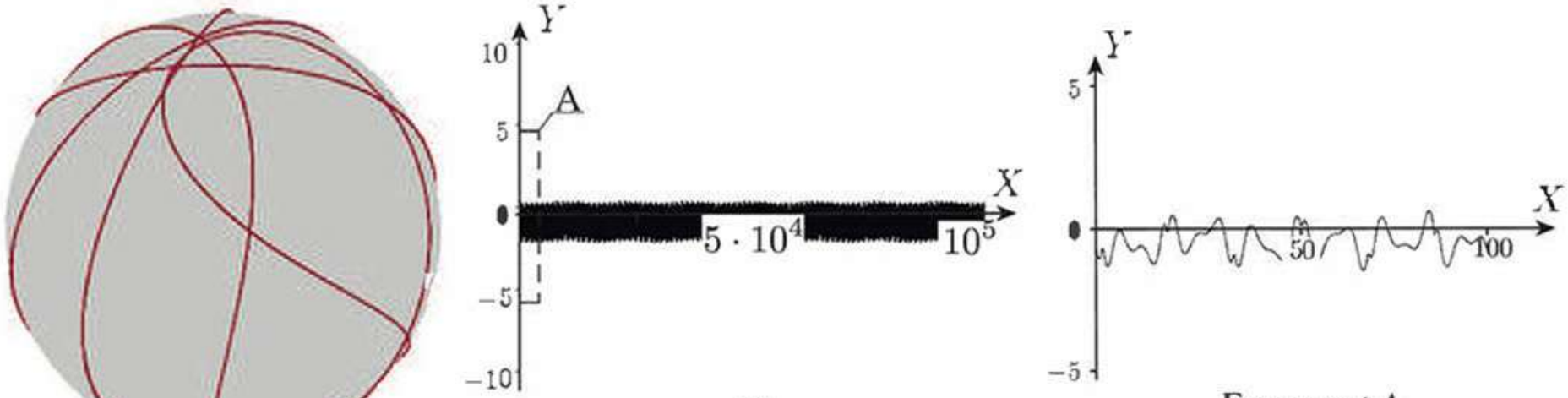

Fig. 20: Projection of the trajectory onto the Poisson sphere and the trajectory of the point of contact for the initial conditions from the neighborhood of the stable fixed point in the Poincaré map in Fig. 11a ($L = 3.6$, $l = 0.6$) and for the initial conditions $X(0) = 0$, $Y(0) = 0$, ($a = 1$).

a)

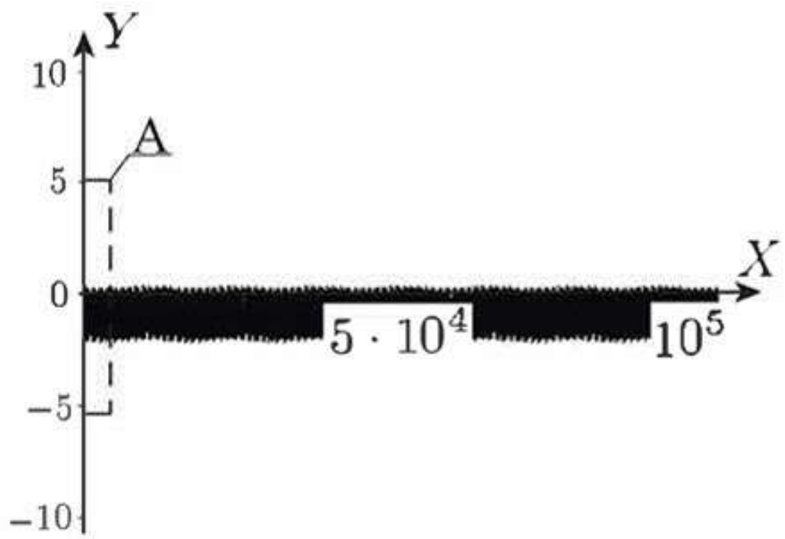

b)

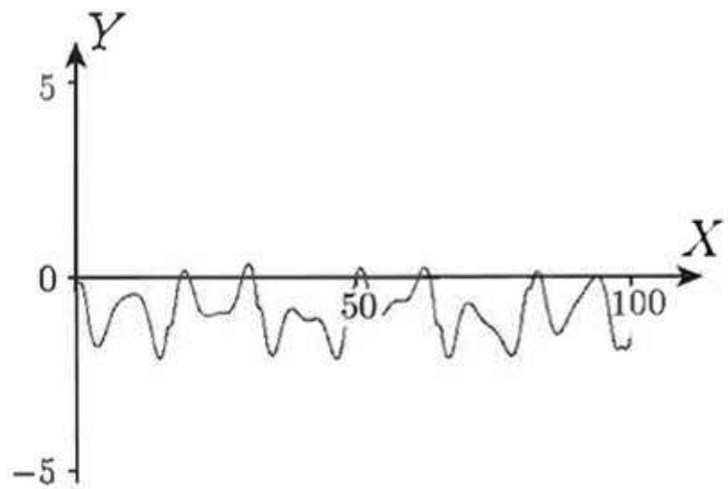

Fragment A

Fig. 21: Projection of the trajectory onto the Poisson sphere and the trajectory of the point of contact for the initial conditions from the neighborhood of the stable limit cycle in the Poincaré map in Fig. 11a ($L = 0, l = 1.96$) and for the initial conditions $X(0) = 0$, $Y(0) = 0$, ($a = 1$).

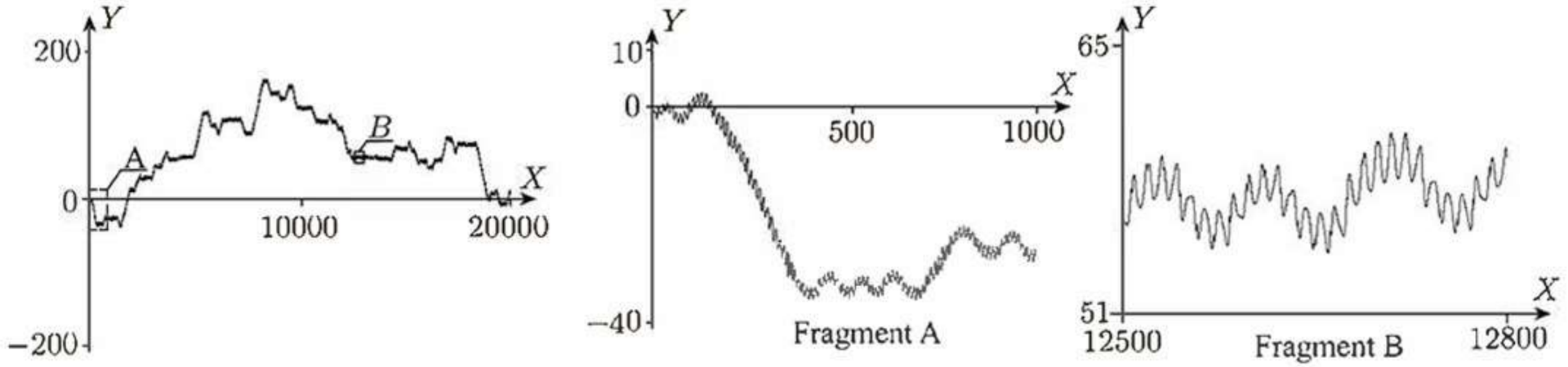

Fig. 22: The trajectory of the point of contact for the initial conditions from the neighborhood of the stable limit cycle in the Poincaré map in Fig. 11b ($L = 0, l = 0.6$) and for the initial conditions $X(0) = 0$, $Y(0) = 0$, ($a = 1$).

References

[1] Artes, J. C., Llibre, J., and Schlomiuk, D., The Geometry of Quadratic Differential Systems with a Weak Focus of Second Order, *Internat. J. Bifur. Chaos Appl. Sci. Engrg.,* 2006, vol. 16, no. 11, pp. 3127–3194.

[2] Balseiro, P. and García-Naranjo, L. C., Gauge Transformations, Twisted Poisson Brackets and Hamiltonization of Nonholonomic Systems, *Arch. Ration. Mech. Anal.,* 2012, vol. 205, no. 1, pp. 267–310.

[3] Bizyaev, I. A., Borisov, A. V., and Mamaev, I. S., Dynamics of the Chaplygin Ball on a Rotating Plane, *Russ. J. Math. Phys.,* 2018, vol. 25, no. 4, pp. 423–433.

[4] Bizyaev, I. A., Borisov, A. V., Kozlov, V. V., and Mamaev, I. S., Fermi-Like Acceleration and Power-Law Energy Growth in Nonholonomic Systems, *Nonlinearity,* 2019, vol. 32, no. 9, pp. 3209–3233.

[5] Bizyaev, I. A., Borisov, A. V., and Mamaev, I. S., Exotic Dynamics of Nonholonomic Roller Racer with Periodic Control, *Regul. Chaotic Dyn.,* 2018, vol. 23, nos. 7–8, pp. 983–994.

[6] Bizyaev, I. A., Borisov, A. V., and Mamaev, I. S., The Chaplygin Sleigh with Parametric Excitation: Chaotic Dynamics and Nonholonomic Acceleration, *Regul. Chaotic Dyn.,* 2017, vol. 22, no. 8, pp. 955–975.

[7] Bolotin, S. V., The Problem of Optimal Control of a Chaplygin Ball by Internal Rotors, *Regul. Chaotic Dyn.,* 2012, vol. 17, no. 6, pp. 559–570.

[8] Bolsinov, A. V., Borisov, A. V., and Mamaev, I. S., Geometrisation of Chaplygin's Reducing Multiplier Theorem, *Nonlinearity,* 2015, vol. 28, no. 7, pp. 2307–2318.

[9] Borisov, A. V. and Fedorov, Yu. N., On Two Modified Integrable Problems in Dynamics, *Mosc. Univ. Mech. Bull.,* 1995, vol. 50, no. 6, pp. 16–18; see also: *Vestnik Moskov. Univ. Ser. 1. Mat. Mekh.,* 1995, no. 6, pp. 102–105.

[10] Borisov, A. V., Fedorov, Yu. N., and Mamaev, I. S., Chaplygin Ball over a Fixed Sphere: An Explicit Integration, *Regul. Chaotic Dyn.,* 2008, vol. 13, no. 6, pp. 557–571.

[11] Borisov, A. V., Ivanova, T. B., Kilin, A. A., and Mamaev, I. S. Nonholonomic Rolling of a Ball on the Surface of a Rotating Cone, *Nonlinear Dynam.,* 2019, vol. 97, no. 2, pp. 1635–1648.

[12] Borisov, A. V., Kilin, A. A., Karavaev, Y. L., and Klekovkin, A. V., Stabilization of the Motion of a Spherical Robot Using Feedbacks, *Appl. Math. Model.,* 2019, vol. 69, pp. 583–592.

[13] Borisov, A. V., Kilin, A. A., and Mamaev, I. S., The Problem of Drift and Recurrence for the Rolling Chaplygin Ball, *Regul. Chaotic Dyn.,* 2013, vol. 18, no. 6, pp. 832–859.

[14] Borisov, A. V., Kilin, A. A., and Mamaev, I. S., Generalized Chaplygin's Transformation and Explicit Integration of a System with a Spherical Support, *Regul. Chaotic Dyn.,* 2012, vol. 17, no. 2, pp. 170–190.

[15] Borisov, A. V., Kilin, A. A., and Mamaev, I. S., How to Control Chaplygin's Sphere Using Rotors, *Regul. Chaotic Dyn.,* 2012, vol. 17, nos. 3–4, pp. 258–272.

[16] Borisov, A. V. and Mamaev, I. S., Two Non-holonomic Integrable Problems Tracing Back to Chaplygin, *Regul. Chaotic Dyn.,* 2012, vol. 17, no. 2, pp. 191–198.

[17] Borisov, A. V. and Mamaev, I. S., *Rigid Body Dynamics,* De Gruyter Stud. Math. Phys., vol. 52, Berlin: De Gruyter, 2018.

[18] Borisov, A. V. and Mamaev, I. S., Symmetries and Reduction in Nonholonomic Mechanics, *Regul. Chaotic Dyn.,* 2015, vol. 20, no. 5, pp. 553–604.

[19] Borisov, A. V. and Mamaev, I. S., Conservation Laws, Hierarchy of Dynamics and Explicit Integration of Nonholonomic Systems, *Regul. Chaotic Dyn.,* 2008, vol. 13, no. 5, pp. 443–490.

[20] Borisov, A. V. and Mamaev, I. S., The Rolling Motion of a Rigid Body on a Plane and a Sphere: Hierarchy of Dynamics, *Regul. Chaotic Dyn.,* 2002, vol. 7, no. 2, pp. 177–200.

[21] Borisov, A. V. and Mamaev, I. S., The Dynamics of the Chaplygin Ball with a Fluid-Filled Cavity, *Regul. Chaotic Dyn.,* 2013, vol. 18, no. 5, pp. 490–496.

[22] Borisov, A. V. and Mamaev, I. S., Obstacle to the Reduction of Nonholonomic Systems to the Hamiltonian Form, *Dokl. Phys.,* 2002, vol. 47, no. 12, pp. 892–894; see also: *Dokl. Akad. Nauk,* 2002, vol. 387, no. 6, pp. 764–766.

[23] Borisov, A. V. and Mamaev, I. S., Chaplygin's Ball Rolling Problem Is Hamiltonian, *Math. Notes,* 2001, vol. 70, nos. 5–6, pp. 720–723; see also: *Mat. Zametki,* 2001, vol. 70, no. 5, pp. 793–795.

[24] Borisov, A. V., Mamaev, I. S., and Bizyaev, I. A., Dynamical Systems with Non-Integrable Constraints: Vaconomic Mechanics, Sub-Riemannian Geometry, and Non-Holonomic Mechanics, *Russian Math. Surveys,* 2017, vol. 72, no. 1, pp. 1–32; see also: *Uspekhi Mat. Nauk,* 2017, vol. 72, no. 5(437), pp. 3–62.

[25] Borisov, A. V., Mamaev, I. S., and Bizyaev, I. A., Historical and Critical Review of the Development of Nonholonomic Mechanics: the Classical Period, *Regul. Chaotic Dyn.,* 2016, vol. 21, no. 4, pp. 455–476.

[26] Borisov, A. V., Mamaev, I. S., and Bizyaev, I. A., The Jacobi Integral in Nonholonomic Mechanics, *Regul. Chaotic Dyn.,* 2015, vol. 20, no. 3, pp. 383–400.

[27] Borisov, A. V., Mamaev, I. S., and Bizyaev, I. A., The Hierarchy of Dynamics of a Rigid Body Rolling without Slipping and Spinning on a Plane and a Sphere, *Regul. Chaotic Dyn.,* 2013, vol. 18, no. 3, pp. 277–328.

[28] Borisov, A. V., Mamaev, I. S., and Kilin, A. A., The Rolling Motion of a Ball on a Surface. New Integrals and Hierarchy of Dynamics, *Regul. Chaotic Dyn.,* 2002, vol. 7, no. 2, pp. 201–219.

[29] Chaplygin, S. A., On a Ball's Rolling on a Horizontal Plane, *Regul. Chaotic Dyn.,* 2002, vol. 7, no. 2, pp. 131–148; see also: *Math. Sb.,* 1903, vol. 24, no. 1, pp. 139–168.

[30] Chaplygin, S. A., On the Theory of Motion of Nonholonomic Systems. The Reducing-Multiplier Theorem, *Regul. Chaotic Dyn.,* 2008, vol. 13, no. 4, pp. 369–376.

[31] Chaplygin, S. A., On Some Generalization of the Area Theorem with Applications to the Problem of Rolling Balls, *Regul. Chaotic Dyn.,* 2012, vol. 17, no. 2, pp. 199–217.

[32] Chaplygin, S. A., On a Pulsating Cylindrical Vortex, *Regul. Chaotic Dyn.,* 2007, vol. 12, no. 1, pp. 101–116.

[33] Chaplygin, S. A., One Case of Vortex Motion in Fluid, *Regul. Chaotic Dyn.,* 2007, vol. 12, no. 2, pp. 219–232.

[34] Ehlers, K. M. and Koiller, J., Rubber Rolling: Geometry and Dynamics of $2-3-5$ Distributions, in *Proc. IUTAM Symposium 2006 on Hamiltonian Dynamics, Vortex Structures, Turbulence (Moscow, Russia, 25–30 August 2006),* pp. 469–480.

[35] Fassò, F., García-Naranjo, L. C., and Sansonetto, N., Moving Energies As First Integrals of Nonholonomic Systems with Affine Constraints, *Nonlinearity,* 2018, vol. 31, no. 3, pp. 755–782.

[36] Fassò, F. and Sansonetto, N., Conservation of "Moving" Energy in Nonholonomic Systems with Affine Constraints and Integrability of Spheres on Rotating Surfaces, *J. Nonlinear Sci.,* 2016, vol. 26, no. 2, pp. 519–544.

[37] Fedorov, Yu. N., Motion of a Rigid Body in a Spherical Suspension, *Vestn. Mosk. Univ. Ser. 1. Mat. Mekh.,* 1988, no. 5, pp. 91–93 (Russian).

[38] Fedorov, Y. N. and Kozlov, V. V., Various Aspects of n-Dimensional Rigid Body Dynamics, *Amer. Math. Soc. Transl. (2),* 1995, vol. 168, pp. 141–171.

[39] Golubev, V. V., *Chaplygin,* Izhevsk: Institute of Computer Science, 2002 (Russian).

[40] Hatcher, A., *Algebraic Topology,* Cambridge: Cambridge Univ. Press, 2002.

[41] Ilin, K. I., Moffatt, H. K., and Vladimirov, V. A., Dynamics of a Rolling Robot, *Proc. Natl. Acad. Sci. USA,* 2017, vol. 114, no. 49, pp. 12858–12863.

[42] Kilin, A. A., Pivovarova E. N., Qualitative Analysis of the Nonholonomic Rolling of a Rubber Wheel with Sharp Edges, *Regul. Chaotic Dyn.,* 2019, vol. 24, no. 2, pp. 212–233.

[43] Kilin, A. A. and Pivovarova, E. N., Chaplygin Top with a Periodic Gyrostatic Moment, *Rus. J. Math. Phys.,* 2018, vol. 25, no. 4, pp. 509–524.

[44] Kozlov, V. V., On the Theory of Integration of the Equations of Nonholonomic Mechanics, *Regul. Chaotic Dyn.,* 2002, vol. 7, no. 2, pp. 191–176.

[45] Kuleshov, A. S., On the Generalized Chaplygin Integral, *Regul. Chaotic Dyn.,* 2001, vol. 6, no. 2, pp. 227–232.

[46] Li, C., Two Problems of Planar Quadratic Systems, *Sci. Sinica Ser. A,* 1983, vol. 26, no. 5, pp. 471–481.

[47] Lichtenberg, A. J., Lieberman, M. A., and Cohen, R. H., Fermi Acceleration Revisited, *Phys. D,* 1980, vol. 1, no. 3, pp. 291–305.

[48] Markeev, A. P., Integrability of the Problem of Rolling of a Sphere with a Multiply Connected Cavity Filled with an Ideal Fluid, *Izv. Akad. Nauk SSSR. Mekh. Tverd. Tela,* 1986, vol. 21, no. 1, pp. 64–65 (Russian).

[49] Putkaradze, V. and Rogers, S., On the Dynamics of a Rolling Ball Actuated by Internal Point Masses, *Meccanica,* 2018, vol. 53, no. 15, pp. 3839–3868.

[50] Svinin, M., Morinaga, A., and Yamamoto, M., On the Dynamic Model and Motion Planning for a Spherical Rolling Robot Actuated by Orthogonal Internal Rotors, *Regul. Chaotic Dyn.,* 2013, vol. 18, nos. 1–2, pp. 126–143.

[51] Tsiganov, A. V., Hamiltonization and Separation of Variables for a Chaplygin Ball on a Rotating Plane, *Regul. Chaotic Dyn.,* 2019, vol. 24, no. 2, pp. 171–186.

[52] Tsiganov, A. V., On the Poisson Structures for the Nonholonomic Chaplygin and Veselova Problems, *Regul. Chaotic Dyn.,* 2012, vol. 17, no. 5, pp. 439–450.